Assessment of the exposure responses to 3R4F smoke and THS 2.2 aerosol in the context of xenobiotic metabolism

TABLE OF CONTENTS

1 ABBREVIATIONS 5

2 INTRODUCTION 6

2.1 The three phases of xenobiotic metabolism 6

2.2 Polymorphisms in genes encoding XMEs and transporters, and disease risk 6

2.3 XMEs and transporters of the respiratory tract 7

2.4 Respiratory tract metabolism and transport of xenobiotic compounds 10

3 DESCRIPTION OF STUDIES THAT COMPARED THE IMPACTS OF 3R4F OR THS2.2 EXPOSURE ON XENOBIOTIC METABOLISM 12

3.1 ApoE-/- mouse switching study 12

3.2 OECD THS 2.2 and mentholated THS 2.2 TG413 studies 12

3.3 Organotypic tissue culture studies 13

4 EXPOSURE RESPONSE TO THS 2.2 AEROSOL OR 3R4F CS MEASURED IN THE CONTEXT OF XENOBIOTIC METABOLISM 13

4.1 Impact of 3R4F and THS 2.2 exposure on liver xenobiotic metabolism in the ApoE-/- mice switching study 13

4.2 Regulation of genes encoding the XMEs and transporters in response to 3R4F or THS 2.2 exposure in respiratory tissues 15

4.2.1 Gene panel 15

4.2.2 Response in rodent lung 16

4.2.3 Response in rodent nasal epithelium 19

4.2.4 Response of organotypic tissue cultures exposed to whole aerosol 21

4.3 CYP activity in response to 3R4F or THS2.2 exposure 23

4.3.1 CYP1A2 activity changes in response to smoking abstinence and switching to THS 2.2 23

4.3.2 CYP1A1/1B1 activity in organotypic cultures in response to 3R4F or THS 2.2 exposure 24

4.4 Activation of the xenobiotic metabolism network in response to 3R4F or THS2.2 exposure 25

4.4.1 Description of the xenobiotic metabolism network model 25

4.4.2 Perturbation of the xenobiotic metabolism network model in response to CS and THS 2.2 exposure in rodent lung 26

4.4.3 Perturbation of the xenobiotic metabolism network model in response to CS or THS 2.2 exposure in rodent nasal epithelium 27

4.4.4 Perturbation of the xenobiotic metabolism network model in response to CS or THS 2.2 exposure in organotypic tissue cultures 29
4.5 Translation of the xenobiotic metabolism response between different experimental systems 30
4.5.1 Response of xenobiotic metabolism to THS 2.2 in pre-clinical models compared with in human studies 30
4.5.2 Comparability of 3R4F CS and THS 2.2 aerosol exposure in the context of the xenobiotic metabolism network 34
5 CONCLUSIONS 37
6 REFERENCES 38

TABLE OF TABLES

Table 1. Panel of genes encoding xenobiotic metabolizing enzymes (XMEs) used to assess the exposure responses. 15

Table 2. Changes in CYP1A2 activity in 5-day clinical studies in Japanese and US populations (full analysis set population) 23

Table 3. Changes in CYP1A2 activity in 3-month clinical studies in Japanese and US populations (full analysis set population) 24

TABLE OF FIGURES

Figure 1. The main xenobiotic metabolizing enzymes and transporters of the respiratory epithelium. 10

Figure 2. Analyses of ApoE-/- mouse liver to determine the impact of CS and THS 2.2 exposure on xenobiotic metabolism. 14

Figure 3. Regulation of genes encoding xenobiotic metabolizing enzymes (XMEs) and transporters in rodent lung. 18

Figure 4. Regulation of genes encoding xenobiotic metabolizing enzymes (XMEs) and transporters in rodent nasal epithelium. 20

Figure 5. Regulation of genes encoding xenobiotic metabolizing enzymes (XMEs) and transporters in organotypic tissue cultures. 22

Figure 6. CYP1A1/CYP1B1 activity in organotypic tissue cultures following exposure to 3R4F and THS 2.2. 25

Figure 7. Structure of the xenobiotic metabolism network model and the principle of scoring the network model with transcriptomics data. 26

Figure 8. Perturbation of the xenobiotic metabolism network in rodent lungs in response to 3R4F or THS 2.2 exposure. 27

Figure 9. Perturbation of the xenobiotic metabolism network in rodent nasal epithelium in response to 3R4F or THS 2.2 exposure. 28

Figure 10. Perturbation of the xenobiotic metabolism network in organotypic tissue cultures in response to CS or THS 2.2 exposure 29

Figure 11. Comparability of the differential network backbone values for the xenobiotic metabolism model from human bronchial brushing datasets and the ApoE-/- mice switching study in response to CS exposure. 31

Figure 12. Comparability of the differential network backbone values for the xenobiotic metabolism network between human smoker bronchial brushings and rat respiratory tissues from the OECD THS 2.2 and OECD THS 2.2M TG413 studies 32

Figure 13. Comparability of the differential network backbone values for the xenobiotic metabolism model between human bronchial brushing datasets and in vitro organotypic cultures in response to smoke exposure. 33

Figure 14. Comparability of the differential network backbone values for the xenobiotic metabolism model in nasal epithelium of ApoE-/- mice exposed to 3R4F or THS 2.2. 34

Figure 15. Comparability of the differential network backbone values for the xenobiotic metabolism model between lungs of rats exposed to 3R4F, 1×MIS, or 2×MIS and lungs of rats exposed to THS 2.2 or THS 2.2M for 90 days. 35

Figure 16. Comparability of the differential network backbone values for the xenobiotic metabolism model in organotypic cultures exposed to 3R4F or THS 2.2. 36

1 ABBREVIATIONS

ABC	ATP-binding cassette
ALDH	Aldehyde dehydrogenase
AHR	Aryl hydrocarbon receptor
BEL	Biological Expression Language
COPD	Chronic obstructive pulmonary disease
CS	Cigarette smoke
CYP	Cytochrome P450
EPHX	Epoxide hydrolase
FMO	Flavoprotein monooxygenase
GST	Glutathione S-transferase
LS	Least-squares
MIS	Menthol in smoke
MRP	Multidrug resistance-associated protein
NAT	Arylamine N-acetyltransferase
NNAL	4-(methylnitrosamino)-1-(3-pyridyl)-1-butanol
NNK	4-(methylnitrosamino)-1-(3-pyridyl)-1-butanone
PAH	Polycyclic aromatic hydrocarbon
SA	Smoking abstinence
THS 2.2	Tobacco heating system 2.2
UGT	UDP-glucuronosyltransferase
XME	Xenobiotic metabolizing enzyme

2 INTRODUCTION

2.1 The three phases of xenobiotic metabolism

Xenobiotic metabolism is the process that converts harmful substances into excretable forms for removal from the body, but can also convert procarcinogenic compounds into more harmful ones (Guengerich, 2000; Guengerich & Shimada, 1998).

The most prominent enzymes in the phase I response to xenobiotics are the cytochrome P450s (also known as CYPs or P450s). CYPs can detoxify or activate xenobiotic compounds by catalyzing chemical reactions, such as oxidation, reduction, or hydrolysis with the aim of making them more water soluble (Omiecinski et al, 2011). Flavoprotein monooxygenases (FMOs) are a superfamily of phase I xenobiotic metabolizing enzymes (XMEs) that are active towards a wide range of xenobiotics. Other important phase I XMEs belong to the aldehyde dehydrogenase (ALDH) superfamily that catalyze the oxidation of exogenous and endogenous aldehydes in a NAD(P)(+)- dependent manner (Marchitti et al, 2008; Vasiliou et al, 2013), and to the aldo-keto reductases (AKRs) that catalyze the oxidation of proximate carcinogenic PAH trans-dihydrodiols (as generated by some CYPs) to yield electrophilic and redox-active PAH o-quinones and can induce redox cycling and reactive oxygen species (ROS) (Petrash, 2013).

In the phase II response, transferase enzymes generally catalyze conjugation reactions such as glucuronidation, sulfation, methylation, and acetylation (Omiecinski et al, 2011). The products of phase II reactions are often more hydrophilic than their parent compounds, making them readily excretable (Omiecinski et al, 2011). Known families of phase II XMEs include UDP-glucuronosyltransferases (UGTs), sulfotransferases, N-acetyltransferases (arylamine N-acetyltransferases, NATs), glutathione S-transferases (GSTs), the NAD(P)H-quinone reductase NQO1, and various methyltransferases (Omiecinski et al, 2011). Most of the substrates of these conjugation reactions are the products of phase I enzymes (Croom, 2012).

The phase III xenobiotic response involves active membrane transporters that transport xenobiotics across the cellular membranes (Croom, 2012; Omiecinski et al, 2011). The initial phase III enzymes were the ATP-binding cassette (ABC) family of drug transporters, but they now include the organic anion transporters and organic cation transporters of the SLC22A superfamily and the organic anion-transporting polypeptides of the SLCO superfamily (Omiecinski et al, 2011).

2.2 Polymorphisms in genes encoding XMEs and transporters, and disease risk

Polymorphisms in the genes encoding the XMEs alter the incidences of cancer and the toxicities derived from chemical exposures (Omiecinski et al, 2011). For example, the CYP2C9 I359L polymorphism affects the 6-hydroxylation of (R)-warfarin and the oxidation of the carbinol moiety on the prodrug losartan (antihypertensive) but not the 4′-hydroxylation of diclofenac (Guengerich, 2003). Although, genotyping can provide useful information about the expected behavior of a drug, large-scale analyses of the single nucleotide polymorphisms (SNPs) in the P450s have been done only in very few clinical trials (Guengerich, 2003). Most identified SNPs in human P450s have been documented in http://www.cypalleles.ki.se/ (Guengerich, 2003). Predicting the catalytic activity of the P450 variants based on homology modeling has not been useful (Guengerich, 2003).

Human observational studies have not shown a clear relationship between the variants of P450 genes and cancer risk (Guengerich, 2003). Nonetheless, early studies have suggested the association between lung cancer risk in smokers and the inducibility of benzo[a]pyrene 3′-hydroxylation by CYP1A1 and CYP1B1 in peripheral blood lymphocytes (Guengerich, 2003). However, the results have been difficult to reproduce and their significance and the mechanism involved remain to be determined (Guengerich, 2003). SNPs in the *CYP2E1* gene, which were analyzed with non-invasive probes (e.g. chlorzoxazone 6-hydroxylation), affected CYP2E1 activity (Guengerich, 2003).

Although AKRs can contribute to genotoxic ROS generation and are involved in the carbonyl reduction of the tobacco-specific nitrosamine, NNK, a recent SNP study found no association between major AKR variants and the lung cancer risk (Modesto et al, 2015); however, AKR1B10 which is a potential biomarker of non-small cell lung cancer (NSCLC) de-activates the anticancer drug, daunorubicin, and its catalytic activity greatly varies in a Cys299Ser mutant (Balendiran et al, 2009).

ALDH2 polymorphisms have been associated with some smoking-related diseases. The inactive ALDH2-2 allele was strongly correlated with secondary esophageal preneoplastic lesions in patients with primary head and neck cancer in Japan (Muto et al, 2002), and in combination with smoking, this allele increased the risk of myocardial infarction and infarct size (Morita et al, 2015). In a recent Japanese pilot study, a significant gene-environment interaction between the ALDH2-2 allele and cumulative exposure to cigarette smoke on the risk of airway obstruction was demonstrated (Morita et al, 2015). A weak association between ALDH2-1-2 polymorphisms and pancreatic cancer was preliminarily evident in a meta-analysis (Mazaki et al, 2011), Polymorphisms of ALDH1 were not associated with increased lung cancer risk in a Chinese case-control study (Wang et al, 2014), and ALDH3A1 polymorphisms have not been associated with smoking related disease risks.

A polymorphic *UGT2B17* gene deletion has been associated with a reduced rate of 4-(methylnitrosamino)-1-(3-pyridyl)-1-butanol (NNAL) detoxification in human liver microsomes (Lazarus et al, 2005) and lung adenocarcinoma risk (Gallagher et al, 2007). Peripheral blood lymphocytes were used to identify polymorphisms in phase II enzymes (i.e. GSTM1, GSTT1, and GSTP1) (Jiao et al, 2007). Blood lymphocytes from non-cancer healthy subjects were cultured within 2 hours of blood collection (Jiao et al, 2007). Significant association was observed between the *GSTT1* null genotype in never smokers and the number of years smoked (Jiao et al, 2007). These observations suggested the role of the *GSTT1* null genotype in the formation and removal of *in vitro* N-ethyl-N-nitrosourea-induced levels of the DNA adduct O^6-ethylguanosine (Jiao et al, 2007).

2.3 XMEs and transporters of the respiratory tract

Although liver is the main organ for xenobiotic metabolism (Benowitz et al, 2009; Oesch-Bartlomowicz et al, 2007), several extra-hepatic tissues, including the respiratory tract, also express genes encoding XMEs and transporters, generally at a lower level than the liver (Somers et al, 2007). The CYP profile of the human lung includes CYP1A1, -1B1, -2A6, -2A13, -2B6, -2C18, -2E1, -2F1, -2J2, -3A5 and -4B1 (Hukkanen et al, 2002; Roos & Bolt, 2005). Moreover, several CYP genes, such as *CYP2A13*, *CYP2F1*, *CYP2S1*, *CYP3A5*, and *CYP4B1*, are preferentially expressed in the lung (Ding & Kaminsky, 2003). The genes encoding the two isoforms of human CYP2A6 and

CYP2A13 are expressed in the epithelial cells of trachea and large airways (Chiang et al, 2012; Su et al, 2000; Su et al, 1996). *CYP2A6* mRNA has also been detected in the small airways (Chiang et al, 2012), and *CYP2E1* mRNA has been detected in normal human bronchial epithelial cells (Runge et al, 2001). In rats exposed to CS for 3 days or 3 weeks, *ALDH3* gene expression was substantially increased in nasal epithelium and lungs (Gebel et al, 2004). Figure 1 provides a summary of the XMEs and transporters that have been detected in the lower respiratory tract at either the RNA or protein level.

Genes encoding phase II XMEs, such as *UGT2A1* and *UGT2A3*, but not *UGT2A2*, are expressed in the lung (Bushey et al, 2011; Bushey et al, 2013). Lung also expresses *UGT2B* genes with *UGT2B11* being the most highly expressed, even higher than in the liver (Jones & Lazarus, 2014).

For the phase III transporters, *MRP1* mRNA has been detected in both normal lung and small cell lung cancer (Thomas et al, 1994), and *MRP2* mRNA was detected on the apical surface of airway epithelial cells (Lundgren et al, 2010). In general, the genes encoding XMEs and membrane transporters seem to be expressed at a higher level in the central airways compared with peripheral airways in humans. Interestingly, in contrast to liver, in lung, genes encoding the phase II GST enzymes, were expressed at a higher level than genes encoding phase I enzymes (Berg et al, 2014).

Many genes encoding XMEs are expressed in lung with a different profile than in liver, and are induced by xenobiotic compounds (Pavek & Dvorak, 2008). For example, *CYP1A1* is expressed at a very low level in extra-hepatic tissues, but can be induced in response to exposure (Bieche et al, 2007). Comparison of smokers and nonsmokers revealed the specific induction of several genes encoding XMEs by smoking. The genes encoding CYP1A1 and CYP1B1 were induced in both bronchoalveolar lavage cells and bronchial biopsies from smokers compared with non-smokers, resulting in increased enzymatic activity. The genes encoding CYP2S1 and GSTP1, were induced only in bronchoalveolar lavage cells and the genes encoding CYP2C9, GSTP1, and GSTA2 were induced only in bronchial biopsies of smokers compared with non-smokers. The genes encoding CYP2B6/7, CYP3A5, and UGT2A1 were repressed only in lavage and genes encoding CYP2J2 and epoxide hydrolase 1 (EPHX1) were repressed in biopsies (Thum et al, 2006). *EPHX1* was induced in bronchoalveolar lavage and repressed in bronchial biopsies from smokers compared with non-smokers. The differential expression of genes encoding XMEs in smokers and non-smokers was accompanied by upregulation of the genes encoding liver receptor X and the glucocorticoid receptor that are known to mediate some of the xenobiotic effects.

At the protein level, CYP1A1, CYP1A2, CYP2A, CYP2B6, CYP2C9, CYP2C19, CYP2D6, CYP2E1, CYP3A4, and CYP3A5 were detected in human lung homogenates (Bernauer et al, 2006), and CYP2S1 was expressed mainly in extra-hepatic tissues, such as the respiratory tract (Bebenek et al, 2012; Rylander et al, 2001). CYP2S1 can metabolize eicosanoids in the absence of both NADPH and NADPH–cytochrome P450 reductase in human cell lines (Bebenek et al, 2012) Immunohistochemical staining of human lung tissue has shown that while CYP1A1 was localized in peripheral parts of the airway, GSTs were produced in ciliated cells of the bronchial epithelium and, to a lesser extent, in the distal airways (Anttila et al, 1993). CYP enzymes are mostly expressed in bronchial and bronchiolar epithelium, Clara cells, type II pneumocytes, and alveolar macrophages in human lung, and expression patterns may vary in animal models (Castell

et al, 2005; Hukkanen et al, 2002). ALDH1A3 and ALDH3A1 were observed by IHC in normal lung pneumocytes, with higher abundance in smokers compared with non-smokers, and strong increases for both isoenzymes were seen in preneoplastic lesions and lung adenocarcinoma and squamous-cell carcinoma (Patel et al, 2008). Acute exposure to CS (3 cigarettes) induced decreased epithelial lining fluid levels of ALDH3A1 in non-diseased individuals but increased ALDH3A1 levels in patients with established COPD (Franciosi et al, 2014). AKR1B10 (retinal reductase) is involved in retinoic acid signaling and is implicated in the pathogenesis of lung cancer (Fukumoto et al, 2005; Penning & Lerman, 2008). Upregulation of, e.g., AKR1C1 together with ALDH3A1, CYP1A1, CYP1B1, and NQO1 was observed in buccal mucosa biopsies and in bronchial brushings of smokers and also following in vitro exposure to TPM from CS, and many of these XME genes were down-regulated again after quitting smoking (Gümüş et al, 2008; Zhang et al, 2008).

The multidrug resistance-associated proteins MRP1 and MRP2 transport the beta-O-glucuronide conjugate of the tobacco-specific carcinogen NNAL (NNAL-O-glucuronide) across the cell membrane (Leslie et al, 2001). MRPs have been detected in the bronchus; however, they have remarkably different cellular localizations depending on the cell type, ranging from basolateral, to apical side, to the entire circumference of the plasma membrane, suggesting specific roles for these proteins in respiratory tissue (Bréchot et al, 1998). Both the multidrug resistance P-glycoprotein and MRP1 have been detected in the bronchial and bronchiolar epithelial layers of human lung (Scheffer et al, 2002) and the possible functions of ABC molecules in the lung has been reviewed based on their expression in different cell types (van der Deen et al, 2005).

Comparison of bronchial epithelium from healthy and chronic obstructive pulmonary disease (COPD) subjects showed a smaller amount of MRP1 in COPD patients (van der Deen et al, 2006). Interestingly, there were no differences in the expression of several genes encoding XMEs and transporters between healthy and COPD subjects (Berg et al, 2014).

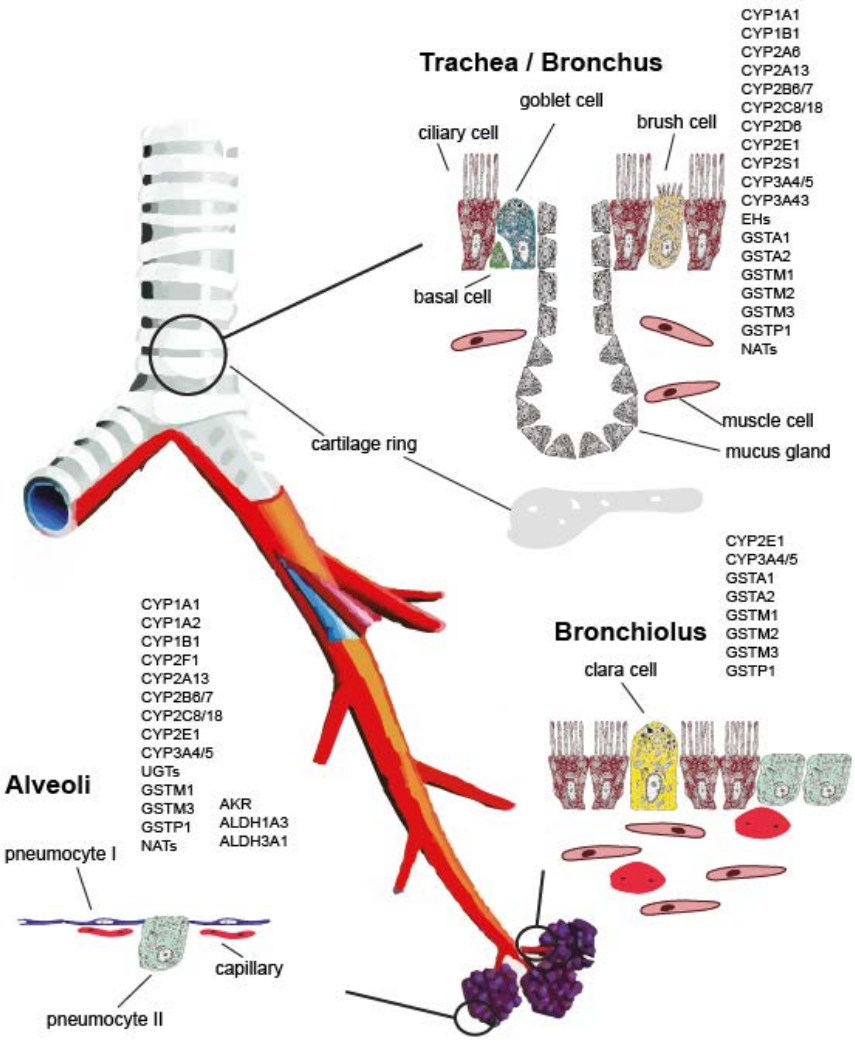


Figure 1. The main xenobiotic metabolizing enzymes and transporters of the respiratory epithelium.

Schematic presentation of the levels of the lower human respiratory tract with the enzymes and transporters that have been detected at the RNA or protein level (Anttila et al, 1993; Zhang et al, 2006).

2.4 Respiratory tract metabolism and transport of xenobiotic compounds

While a body of information exists on the gene expression and regulation of genes encoding the XMEs, less is known about the actual biotransformation of xenobiotic compounds in the lung. Several lung cell types can process xenobiotic compounds to produce reactive metabolites (Gerde et al, 1998; Hecht, 1999). Rodent respiratory tissues seem to have a high capacity to biotransform certain xenobiotics, whereas the human lung has a lower capacity (Dahl & Lewis, 1993). CYP1A1 activity is induced in pulmonary alveolar macrophages of smokers compared with nonsmokers (Cantrell et al, 1973), and Clara cells are particularly responsive to inducers of CYP1A1 and CYP1B1 (Chang et al, 2006). To close the data gap regarding enzymatic activation of CYPs in lung, Bernauer et al established a panel of CYPs to quantify these enzymes in human lung samples and demonstrated CYP1A-related and CYP2E1-specific enzyme activities

in lung tissue (Bernauer et al, 2006). The activities of CYP1A1/1B1 and CYP2A6/2A13 can be measured and maintained in organotypic tissue cultures derived from human tracheobronchial epithelial cells (Baxter et al, 2015; Newland et al, 2011).

Among all of the ALDH superfamily members, ALDH3A1 mRNA levels showed the greatest induction in response to CS extract (CSE) exposure of primary human bronchial epithelial cells (HBECs), and its enzymatic activity was increased in immortalized HBECs; moreover, its overexpression decreased DNA damage and cytotoxicity, while its knockdown increased cytotoxicity of the CSE exposure (Jang et al, 2014).

NATs are conjugating enzymes that were shown to be active in bronchial and alveolar cells, and their activity can be inhibited with oxidants that cause lung dysfunction (Dairou et al, 2009). The direct protective effect of GSTP1 has been demonstrated in lung fibroblast cells exposed to cigarette smoke (CS) condensate, using sense and antisense vector approaches (Ishii et al, 2001). While UGT2A1, which metabolizes PAHs, was active against all PAHs tested (Bushey et al, 2011), UGT2A3 activity was limited to simple PAHs such as 1-OH-pyrene and 1-naphthol (Bushey et al, 2013). Low levels of UGT2B7 mRNA were detected in human lung specimens, and while both UGT2B7 and UGT1A9 play important roles in the overall glucuronidation of NNAL in humans, UGT2B7 potentially plays an important role in the detoxification of NNAL in the lung (Ren et al, 2000).

Because many of the XMEs are induced and expressed at high levels in lung, it has been assumed that some biotransformation will occur at this internal–external interface of the body (Gundert-Remy et al, 2014). For short-lived active metabolites in particular, local metabolism from the parent compound is needed in tissues such as lung (Cohen, 1990; Pelkonen et al, 2008). In support of xenobiotic metabolism-induced target tissue toxicity, rat studies have shown that metabolic activation of 4-(methylnitrosamino)-1-(3-pyridyl)-1-butanone (NNK) via the liver is not required and that bioactivation in the lung leads to DNA damage (Maertens et al, 2010). Mouse models with specific deletion of the NADPH–cytochrome P450 reductase gene in the lung or liver have shown that pulmonary P450 is needed for the production of carcinogenic metabolites and NNK-induced lung tumor formation, and that hepatic P450 is responsible for the clearance of NNK, thereby protecting the lung against NNK-induced carcinogenesis (Weng et al, 2007). The so-called humanized mouse models, which have the endogenous *cyp2a5* gene inactivated and can overexpress various human homologs, have shown that CYP2A13 and/or CYP2F1 can mediate NNK-induced lung tumorigenesis in vivo (Megaraj et al, 2014).

Although nicotine is almost completely absorbed by the respiratory and alveolar epithelium, it is metabolized predominantly in the liver by CYP2A6 (Benowitz et al, 2009). Some biotransformation of nicotine also occurs in lung microsomes with CYP2A13 being the major nicotine-metabolizing enzyme (DeVore & Scott, 2012; Foth, 1995; Foth et al, 1991; Mattammal et al, 1987; Shigenaga et al, 1988). In addition, induction of CYP1A1 in response to nicotine has been shown to occur in lung (Iba et al, 1999; Phillips et al, 2015a; Price et al, 2004).

PAHs can be activated via a number of mechanisms and the enzymatic pathways involved in the activation of PAHs include CYP1A1/1B1 and the epoxide hydrolase pathway, the CYP peroxidase pathway, and the aldo-keto reductase pathway (Moorthy et al, 2015). PAHs induce pulmonary *CYP1A1* expression (Choudhary et al, 2003; Moorthy

et al, 2015), and benzo[*a*]pyrene treatment can induce Cyp1a enzyme activity in mouse lung (Arlt et al, 2015). Lung PAH metabolism of the numerous polycyclic aromatic hydrocarbons (PAHs) produced during tobacco combustion and inhaled by smoking is achieved by pulmonary CYPs, particularly CYP1A1, leading to reactive intermediates and bulky DNA adducts that have been associated with lung cancer risk and can serve as biomarkers (Bartsch et al, 1995; Moorthy et al, 2015). In addition, gastrointestinal uptake and metabolism in the intestine and liver of PAHs ingested from dietary sources such as broiled meat, and also from that fraction of smoke-derived PAHs that is swallowed generates genotoxic metabolites that reach the lung via the pulmonary circulation and contribute to DNA adduct formation (Moorthy et al, 2015). In contrast to the lung, the liver as a major site of PAH metabolism appears not to be a favored target organ for PAH carcinogenesis, although PAH adducts are also formed in hepatic tissue (Kondraganti et al, 2003), hence it may only in part be due to the efficient tissue-specific CYP1 – related detoxification pathways that were seen in intestinal and liver tissue (Nebert et al, 2013). Moreover, phase III (transporter) activity such as MRP4 can reduce the amount of DNA adducts in response to the proximate carcinogen of benzo[a]pyrene, as was demonstrated in functional assays in human lung cells (Gelhaus et al, 2012). An inter-disciplinary approach with systems biologists, epidemiologists, pathologists, omics researchers, mechanistic researchers, and biostatisticians may be required to increase the mechanistic understanding of PAH effects (Moorthy et al, 2015).

3 DESCRIPTION OF STUDIES THAT COMPARED THE IMPACTS OF 3R4F OR THS2.2 EXPOSURE ON XENOBIOTIC METABOLISM

3.1 ApoE-/- mouse switching study

In the ApoE-/- mice switching study, the hallmarks of COPD and cardiovascular disease and general exposure effects were investigated over an 8-month period in response to CS from a combustible reference cigarette (3R4F) or the aerosol of tobacco heating system 2.2 (THS 2.2), a prototype modified risk tobacco product. The nicotine concentrations in both exposure atmospheres, THS 2.2 and 3R4F, were matched at 29.9 µg nicotine /l (equivalent to 600 mg total particulate matter /m^3 for the mainstream smoke from 3R4F). To model the effects of smoking cessation and switching to THS 2.2, mice were first exposed to CS from 3R4F for 2 months and then switched to air or to THS 2.2 aerosol, respectively, for up to 6 additional months. A systems toxicology approach was used to investigate the exposure effects using conventional toxicology parameters, such as physiology and histology, combined with transcriptomics, lipidomics, and proteomics (Phillips et al, 2015b).

3.2 OECD THS 2.2 and mentholated THS 2.2 TG413 studies

In accordance with OECD guideline TG413, we conducted a sub-chronic 90-day inhalation study (Rat-THS-TG413) with THS 2.2 and 3R4F to compare the toxicities of the regular and mentholated 3R4F and THS 2.2 products (Rat-THSM-TG413). For this purpose, rats were exposed to filtered air (sham), or to a low, medium, or high dose of 3R4F corresponding to 8, 15, and 23 µg nicotine /l, respectively, or to a low, medium, or high dose of THS 2.2 corresponding to 15, 23, and 50 µg/l nicotine, respectively.

3.3 Organotypic tissue culture studies

For the *in vitro* assessment of inhaled agents, organotypic airway epithelial models were selected because they are cultured at the air-liquid interface and better resemble airway tissue *in vivo*. The organotypic tissue culture models used were: human bronchial epithelia MucilAir™ (Epithelix Sàrl) and EpiAirway™ (MatTek), human nasal MucilAir™ (Epithelix Sàrl), and human buccal EpiOral™ (MatTek) cultures derived from non-diseased, non-smoking donors.

Using a SM 2000 smoking machine, smoke or aerosol was generated from 3R4F and THS 2.2, respectively, and applied to the organotypic bronchial, nasal, and buccal tissue cultures using a Vitrocell® system. The organotypic tissue cultures were exposed for 28 min to 3R4F CS or THS 2.2 aerosol at the comparable nicotine concentrations and harvested after various post-exposure time points for assessment of the xenobiotic metabolism response.

4 EXPOSURE RESPONSE TO THS 2.2 AEROSOL OR 3R4F CS MEASURED IN THE CONTEXT OF XENOBIOTIC METABOLISM

4.1 Impact of 3R4F and THS 2.2 exposure on liver xenobiotic metabolism in the ApoE-/- mice switching study

Being the main organ for the metabolism of xenobiotic compounds, the livers of ApoE-/- mice exposed to CS and THS 2.2 were analyzed for gene expression and proteomic changes. The gene set enrichment analysis showed that xenobiotic metabolism was one of the most impacted functions based on the proteomics and transcriptomics data (Figure 2A). To gain further insights into the effects of CS exposure on xenobiotic metabolism in liver, a comprehensive panel of xenobiotic proteins/genes was evaluated (Lo Sasso et al, 2016). Several proteins including those involved in phase I (CYPs) and phase II (GSTs, UGTs) reactions were significantly upregulated upon CS exposure. A number of GSTs showed increased abundance in the 3R4F group compared with the sham group (Figure 2B). In contrast to the 3R4F group, in the THS 2.2, cessation, and switching groups no significant increases in the abundance of these or any other xenobiotic enzymes were detected. These data confirmed that CS exposure activated the production of enzymes involved in phase I and II detoxification processes. No significant impact on the induction of these enzymes was observed following THS 2.2 exposure, or after cessation or switching.

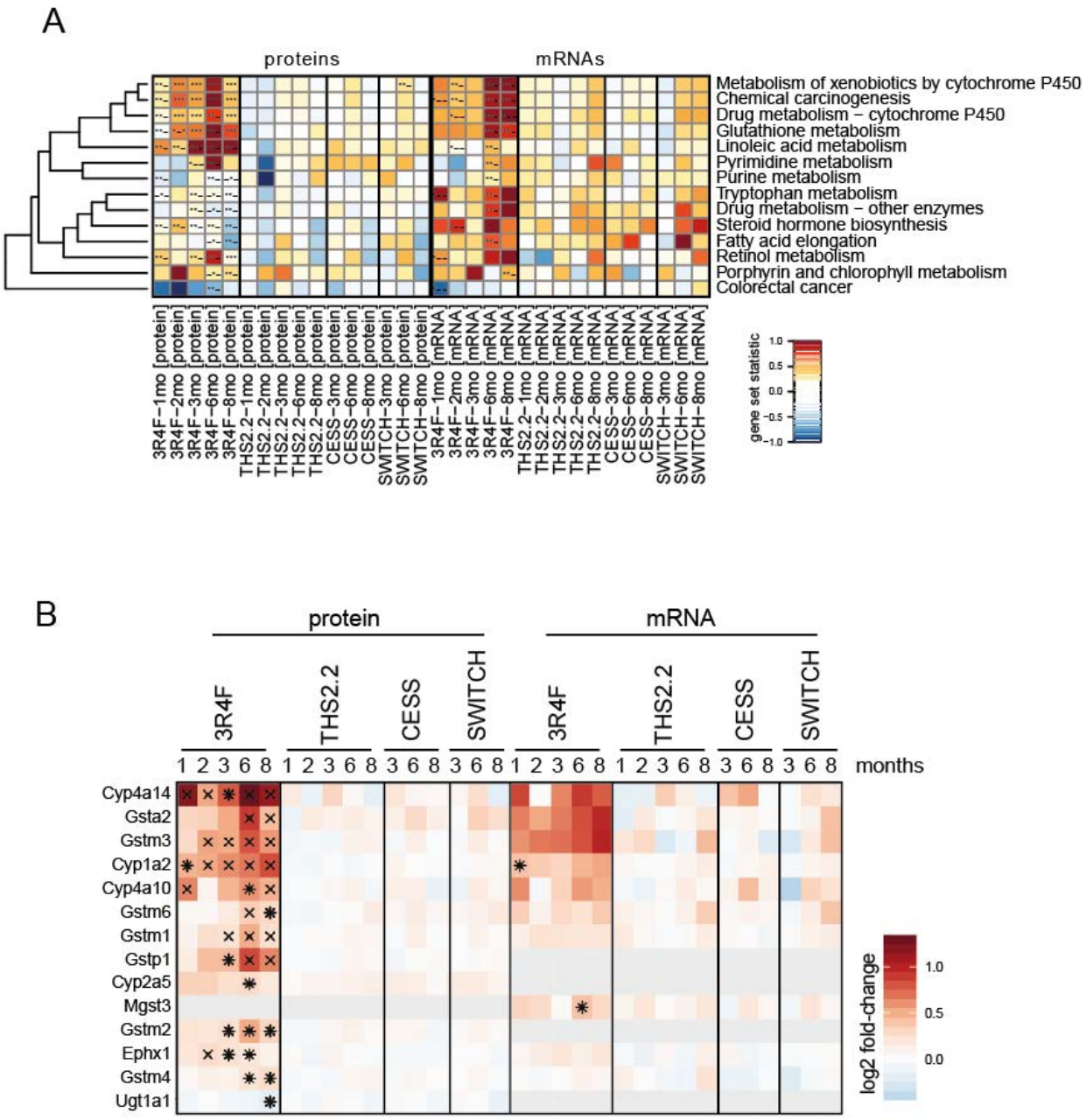


Figure 2. Analyses of ApoE-/- mouse liver to determine the impact of CS and THS 2.2 exposure on xenobiotic metabolism.

A) Protein and gene set enrichment analyses. Set enrichment was assessed by over-representation analysis (ORA) and gene set analysis (GSA). For GSA, fold change compared with sham exposure was used as the protein-level statistic, the mean was used as the set statistic, and sample permutation (Q2) was used to assess statistical significance. The enrichment results were normalized per pathway. Significant differences are indicated by asterisks (*BH-adjusted p-value <0.05). In each square, the first asterisk represents the overall adjusted Fisher p-value of the GSA and ORA analyses, the second asterisk represents the GSA, and the third asterisk represents the ORA results. Significantly affected pathways (BH-adjusted p-value <0.05) in the comparisons of both the proteomics and transcriptomics data are shown. B) CS exposure induced a xenobiotic/oxidative stress response in the liver of ApoE-/-mice. Profiles for significantly affected xenobiotic/oxidative stress proteins/genes are shown (BH-adjusted p-value <0.05). Proteins/genes identified by functional clustering (in A) and extended by the metabolism of xenobiotics in the cytochrome P450 pathway from the KEGG database are included (Kanehisa et al, 2014). The fold changes compared

with the respective sham groups are color-coded and statistically significant differences are marked (BH-adjusted p-value, * <0.05, x <0.01). Missing values are indicated in grey.

4.2 Regulation of genes encoding the XMEs and transporters in response to 3R4F or THS 2.2 exposure in respiratory tissues

4.2.1 Gene panel

We used gene expression analyses by employing the Affymetrix technology conducted from respiratory tissue samples to monitor the induction/repression of genes encoding certain XMEs and transporters in response to 3R4F and THS 2.2 exposure. The panel of genes is shown in Table 1. The panel was adapted from (Garcia-Canton et al, 2013) and augmented with additional genes encoding XMEs relevant in the lung context (Olsson et al, 2011) as well as the aldehyde dehydrogenase genes. While this approach cannot provide insights into the actual metabolic activities in the tissues, it shows that the upstream signaling pathways that lead to regulation of the genes were impacted by the exposures.

Table 1. Panel of genes encoding xenobiotic metabolizing enzymes (XMEs) used to assess the exposure responses.

Phase I	Phase I continued	Phase II	Transporters/Phase III
AKR1B10	CYP2S1	COMT	ABCB1
AKR1C1	CYP1A1	DCXR	ABCC1
AKR1C2	CYP1A2	GST	ABCG2
AKR1C3	CYP1B1	GSTA1	SLC15A2
AKR7A3	CYP1F1	GSTA2	SLC22A1
ALDH16A1	CYP2A13	GSTM1	SLC22A2
ALDH18A1	CYP2A6	GSTP1	SLC22A3
ALDH1A1	CYP2B6	GSTT1	SLC22A4
ALDH1A2	CYP2B7	NAT1	SLC22A5
ALDH1A3	CYP2B7P1	SULT1A1	SLCO2B1
ALDH1B1	CYP2C	UGT1A1	SLCO3A1
ALDH1L1	CYP2C19	UGT1A10	SLCO4A1
ALDH1L2	CYP2C9	UGT1A4	SLCO4C1
ALDH2	CYP2D6	UGT1A6	
ALDH3A1	CYP2E1	UGT1A7	
ALDH3A2	CYP2F1	UGT1A8	
ALDH3B1	CYP2J2	UGT1A9	
ALDH3B2	CYP2S1	UGT2A1	
ALDH4A1	CYP3A4	UGT2A3	

(table continues)

Phase I	Phase I continued	Phase II	Transporters/Phase III
ALDH5A1	CYP3A5	UGT2B10	
ALDH6A1	CYP4B1	UGT2B11	
ALDH7A1	EPHX1	UGT2B7	
ALDH8A1	FMO3		
ALDH9A1	HSD11B1		
AOX1	NQO1		
CBR1			

AKR, aldo-keto reductase; ALDH, aldehyde dehydrogenase; AOX, aldehyde oxidase; CBR, carbonyl reductase; CYP, cytochrome P450; EPHX, epoxide hydrolase; FMO, flavoprotein monooxygenase; HSD, hydroxysteroid dehydrogenase; NQO, NAD(P)H-quinone dehydrogenase; COMT, catechol-O-methyltransferase; DCXR, dicarbonyl L-xylulose reductase; GST, glutathione S-transferase; NAT, N-acetyltransferase; SULT, sulfotransferase; UGT, UDP-glucuronosyltransferase ; ABC, ATP-binding cassette; SLC, solute carrier family; SLCO, solute carrier organic anion transporter.

4.2.2 Response in rodent lung

The gene expression panel described above was constructed from the Affymetrix data produced from lung tissue of rodents exposed to 3R4F CS or THS 2.2 aerosol. Figure 3 shows the results from the ApoE-/- mouse switching study. Only *Slco2b1* and *Akr1b8* were upregulated at 1 month after exposure to 3R4F CS with stronger upregulation in the lungs of mice exposed for 6 or 8 months. The *Cyp1a1*, *Cyp1b1*, and *Slc22a4* genes were upregulated in mouse lungs after 2 months of CS exposure, and *Cyp1a1* was the only gene that showed steadily increased upregulation in the groups that were exposed for 3, 6, and 8 months. *Nqo1* was upregulated only in the groups of mice exposed to CS for 6 and 8 months, and the upregulation of *Ephx1*, *Cbr1*, and *Akr7a5* was significant only in lungs of mice exposed to CS for the full 8 months. Only a very weak upregulation in response to 3R4F exposure was observed at the 8 month time point in genes encoding Aldh9a1, Aldh3b1, Aldh1l1, Aldh16a1, and Aldh18a1.

The *Hsd11b1*, *Cyp2j9*, *Slc22a5*, and *Sult1a1* genes were downregulated only in the lungs of mice exposed to 3R4F for 8 months. *Fmo3* and *Cyp2f2* were downregulated at 6 months, and *Slc22a3* was downregulated at all exposure time points from 2 months onward. Similar but opposite to *Cyp1a1*, *Cyp4b1* was significantly downregulated at 2, 6, and 8 months. *Aox1* and *Slc15a2* were downregulated only at 6 and 2 months, respectively. *Aldh6a1* and *Aldh1a7* genes were downregulated at 2, 6, and 8 month and 6 and 8 month time point, respectively. None of the genes encoding XMEs and transporters that were regulated in response to 3R4F exposure were regulated in lung from the cessation, switching, or THS 2.2 exposure groups.

Unlike in the ApoE-/- mouse, *Cyp1a1* was upregulated in both male and female rat lungs also in response to THS 2.2 and mentholated THS 2.2 (THS 2.2M) exposure (Figure 3), but was not regulated in any of the recovery groups. *Cyp4ba* was downregulated in the lungs of female and male rats exposed to both 3R4F and mentholated reference cigarette (MIS) with slight downregulation also in lungs from male rats exposed to the high doses

of nicotine in the THS 2.2 aerosol for 90 days. The *Akr1c3*, *Dcxr*, and *Nqo1* genes were upregulated in both female and male rat lungs in response to exposure to 3R4F and MIS 3R4F. No regulation was observed in the lung of rats in the recovery groups. *Comt* upregulation was restricted to the lungs of female rats exposed to MIS 3R4F.

Aldh16a1 was induced only in the lungs of female rats in response to 3R4F exposure. *Aldh3b1* and *Aldh4a1* were upregulated in response to both 3R4F and mentholated reference cigarette exposure and the upregulation of the latter was observed also in the lungs of female rats in the recovery group after exposure to the mentholated reference cigarette. *Aldh1l1* and *Aldh7a1* were induced in the female and male rat lung only in response to exposure to the mentholated reference cigarette. Exposure to THS 2.2 didn't induce any regulation of genes encoding aldehyde dehydrogenases (Figure 3).

The weak response in the *Aldh* gene expression may be due to the sample collection time that was up to 20 hours after the last exposure. It has been previously reported that CS-induced changes in aldehyde dehydrogenase genes was seen in rats immediately after end of the 3-weeks exposure and these changes were not clearly observed when tissues were collected 20 h after end of exposure (Gebel et al, 2004).

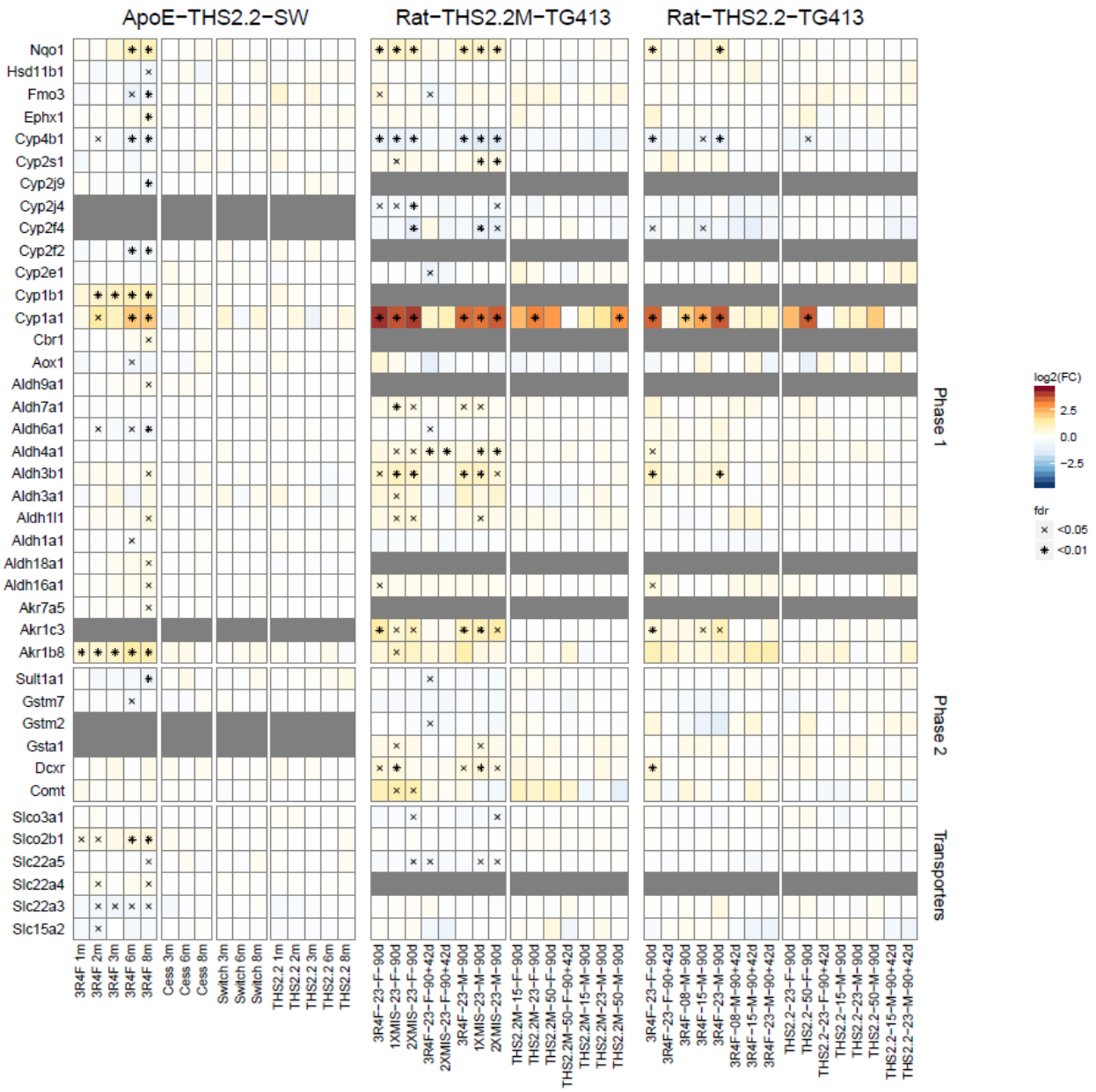


Figure 3. Regulation of genes encoding xenobiotic metabolizing enzymes (XMEs) and transporters in rodent lung.

The heatmaps show the up- or downregulation of genes in the lungs of mice or rats from different exposure groups. The color keys on the right sides of the heatmaps indicate the log2 fold change compared with the expression level in the sham group at corresponding time points. The significance of the fold change is indicated as x for false discovery rate (FDR) <0.05 and * for FDR <0.01. The gene names are as given in Table 1. ApoE-/- mouse switching study: The lanes are labeled with the product (3R4F or THS 2.2) and the timepoint is indicated after the exposure group (1m indicates 1 month, 2m indicates 2 months, and so on). OECD THS 2.2 and OECD THS 2.2M TG413 studies: The lanes are labeled as [product (3R4F or THS 2.2)-nicotine concentration (mg/l)-sex (F, female; M, male)-exposure time point (90d, 90 days; 90+42d, 90 days of exposure with 42 day recovery)]. MIS, menthol in smoke of 3R4F. Only the genes that showed regulation in at last one contrast (exposed vs. control) are shown.

4.2.3 Response in rodent nasal epithelium

The results from the ApoE-/- mouse switching study showed that very few genes encoding XMEs and transporters were impacted, and all the impacted genes were upregulated in response to CS exposure (Figure 4). The *Aldh9a1*, *Aldh1a1*, *Nqo1*, *Hsd1*,*1b1*, *Ephx1*, *Cyp1b1*, and *Dcxr* genes were upregulated at 6 and 8 months, and *Cyp3a13*, *Cyp1a1*, *Aox1*, *akr1b8*, *Slc22a4*, *Slc15a2*, and *Abcg2* were only weakly upregulated with significant differences compared with the sham group apparent at only one time point in response to 3R4F exposure. *Aldh16a1* and *Aldh1a3* were only upregulated at 6 month or 8 month time point, respectively. None of the genes encoding the XMEs or transporters were observed regulated in the nasal epithelium of mice in the THS 2.2, cessation, or switching groups.

In rat nasal epithelium, many genes were regulated in response to 3R4F exposure at 90 days and some were also impacted in the recovery groups (Figure 4). *Hsd11b1*, *Cyp2s1*, *Akr1b8*, *Gstp1*, and *Comt* were regulated also in response to THS 2.2M exposure, but only in female rats and only at the highest nicotine concentration (50 μg/l). *Cyp2s1* was regulated only by THS 2.2M and not by 3R4F.

In both female and male rat nasal epithelium, upregulation was observed for the genes encoding *Aldh3a1* and *Aldh7a1*, in response to both 3R4F and the mentholated reference cigarette. The female recovery group after exposure to the mentholated reference cigarette also showed upregulation of these genes. *Aldh1l2* and *Aldh1a7* showed a similar response to smoke exposure, however, no upregulation could be observed in the recovery groups. *Aldh3a2* and *Aldh2* were weakly downregulated in the rat nasal epithelium in response to smoke exposure, and this regulation was observed also in the female recovery group (Figure 4).

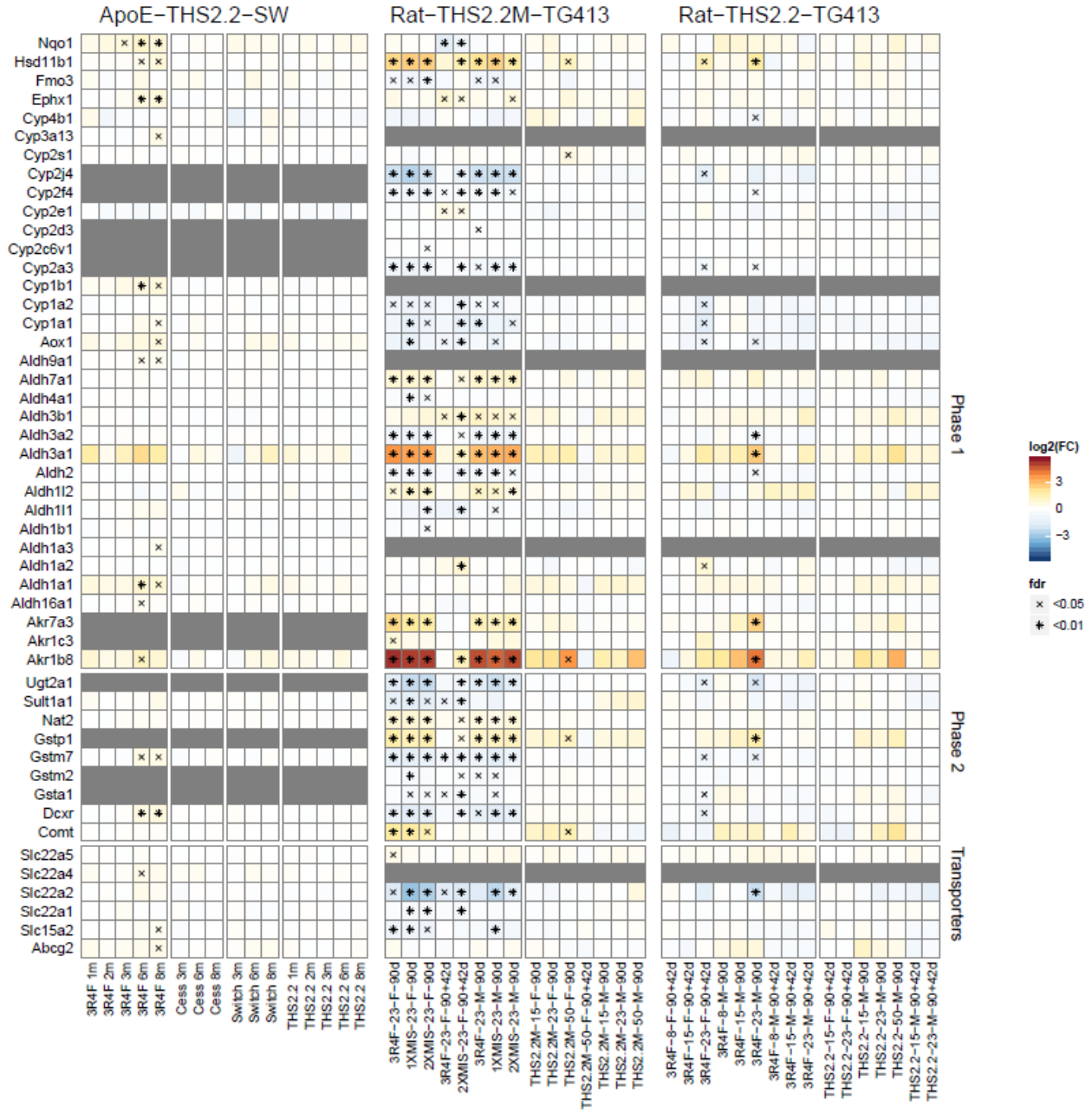


Figure 4. Regulation of genes encoding xenobiotic metabolizing enzymes (XMEs) and transporters in rodent nasal epithelium.

The heatmaps show the up- or downregulation of the genes in the nasal epithelium of mice and rats from different exposure groups. The color keys on the right sides of the heatmaps indicate the log2 fold change compared with the expression level in the sham group at corresponding time points. The significance of the fold change is indicated as x for false discovery rate (FDR) <0.05 and * for FDR <0.01. The gene names are as given in Table 1. ApoE-/- mouse switching stud: The lanes are labeled with the product (3R4F or THS 2.2) and the timepoint is indicated after the exposure group (1m indicates 1 month, 2m indicates 2 months, and so on). OECD THS 2.2 and OECD TG413 THS 2.2M TG413 studies: The lanes are labeled as [product (3R4F or THS 2.2)-nicotine concentration (mg/l)-sex (F, female; M, male)-exposure time point (90d, 90 days; 90+42d, 90 days of exposure with 42 day recovery)]. MIS, menthol in smoke 3R4F. Only the genes that showed regulation in at last one contrast (exposed vs. control) are shown.

4.2.4 Response of organotypic tissue cultures exposed to whole aerosol

The majority of the genes encoding XMEs and transporters were regulated at a higher level in response to 3R4F compared with THS 2.2 in all three organotypic tissue cultures (Figure 5). A small number of genes were regulated only in response to THS 2.2 exposure, including *CYP2J2* in the bronchial, *CYP2E1* in buccal and nasal, and *CYP2C19* and *NAT1* in the nasal organotypic tissue. In addition to xenobiotic metabolism, CYP2J2 was found to be involved in arachidonic acid metabolism (Xu et al, 2013) and may be protective against oxidative stress (Chen et al, 2014). CYP2E1 is known to be induced by ethanol in cultured respiratory epithelial cells (Runge et al, 2001), and the number of CYP2E1-positive cells was found to be increased (similarly to CYP1A1- and CYP2A6-positive cells) in bronchial epithelium of heavily smoking lung cancer patients (Oyama et al, 2006). The CYP2C19-catalyzed two-electron oxidation reaction has been demonstrated in the bioactivation of oxymetazoline to form p-quinone methide species (Mahajan et al, 2011).

Most genes encoding aldehyde dehydrogenases that were tested were regulated by whole 3R4F smoke in the three organotypic tissue cultures. Generally, the response was much weaker or was not observed in response to THS 2.2 exposure. *ALDH1A3*, *ALDH3A1*, and *ALDH8A1* were upregulated in all three tissue cultures in response to 3R4F and THS 2.2 exposure. *ALDH3A2* was strongly upregulated in the buccal tissue in response to 3R4F and THS 2.2, and while *ALDH3B1* was downregulated in the bronchial and nasal cultures in response to 3R4F exposure, it was upregulated in buccal tissue in response to both 3R4F and THS 2.2 exposure. *ALDH5A1* and *ALDH9A1* were weakly downregulated in in all three tissue cultures in response to 3R4F exposure and slightly downregulated in response to THS 2.2 exposure only in the buccal tissue (Figure 5).

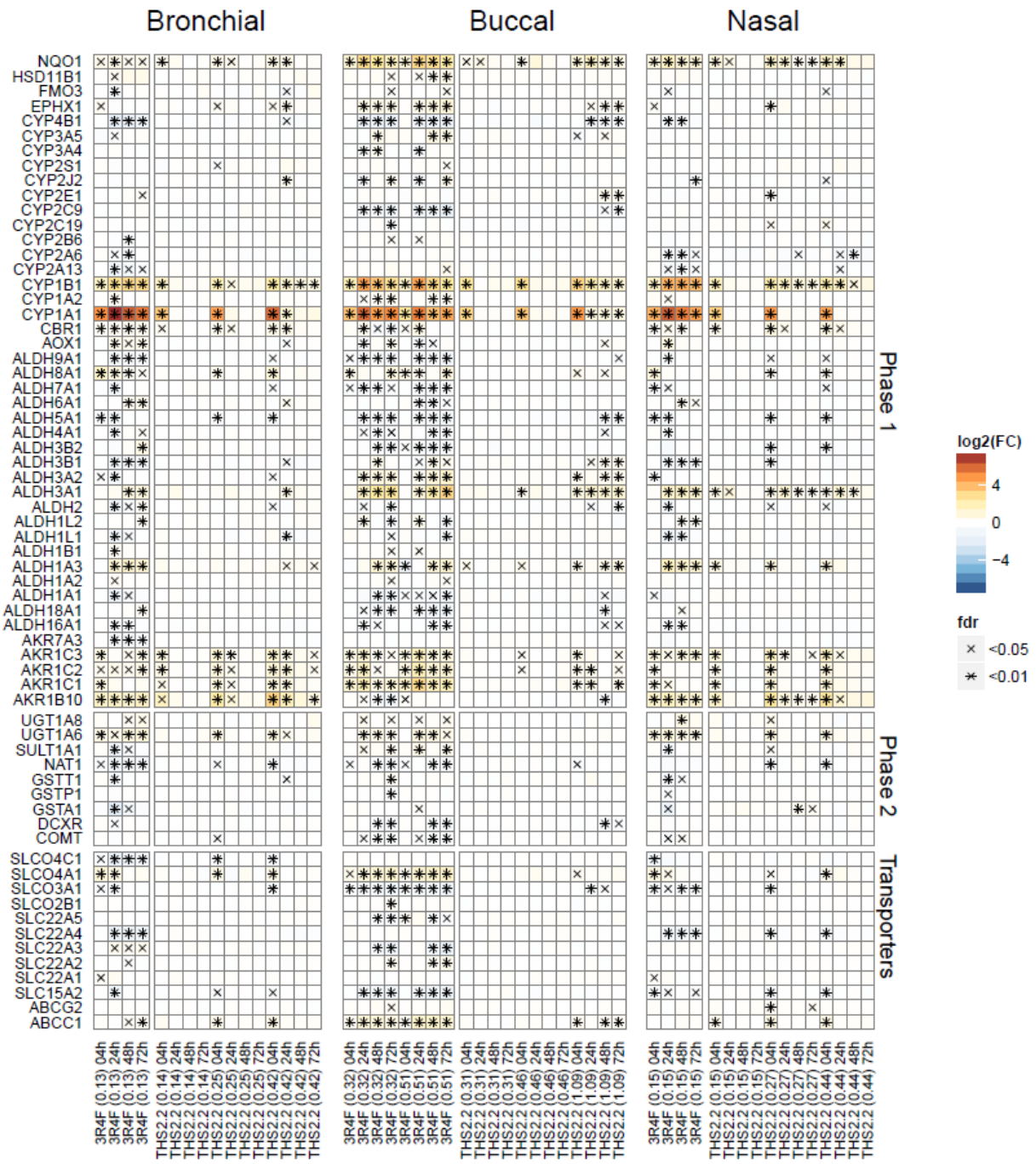


Figure 5. Regulation of genes encoding xenobiotic metabolizing enzymes (XMEs) and transporters in organotypic tissue cultures.

The gene names are as given in Table 1. The color key on the right side of the heatmaps indicates the log2 fold change compared with the expression level in the sham group at corresponding time points. The significance of the fold change is indicated as x for false discovery rate (FDR) <0.05 and * for FDR <0.01. The lanes are labeled with the products (3R4F or THS 2.2) followed by the nicotine concentration (mg/l in parenthesis) and the post exposure time point. Only the genes that showed regulation in at last one contrast (exposed vs. control) are shown.

4.3 CYP activity in response to 3R4F or THS2.2 exposure

4.3.1 CYP1A2 activity changes in response to smoking abstinence and switching to THS 2.2

In our clinical program, special attention was given to CYP1A2 activity changes. The time response of CYP1A2 activity upon smoking cessation was published previously using caffeine as the CYP1A2 substrate (Faber & Fuhr, 2004). The initial caffeine clearance [also called caffeine metabolic ratio (CMR)] estimated from paraxanthine/caffeine plasma ratios, decreased by approximately 36% upon smoking cessation with an apparent 38 hour decrease in the half-life of CYP1A2 activity (Faber & Fuhr, 2004). Using the same approach, changes in CYP1A2 activity were assessed in 5-day (day 5 vs. baseline) and 3-month (day 5 and day 90 vs. baseline) clinical studies in Japanese and US populations. At the baseline, the average CMR was lower in the Japanese study than in the US study (geometric means about 70–74% and 114–121% respectively). This difference was in line with published data (Myrand et al, 2008). After 5 days of exclusive THS 2.2 use, CMR levels decreased significantly and to a similar extent as the CMR levels upon smoking abstinence in all the clinical studies (see Table 2 and Table 3), with a difference for THS 2.2 vs. CS of between 21.7% and 37%. The CMR levels remained low in THS 2.2 users at 3 months in the Japanese study, while the effect was partially diluted in the US study (see Table 3). Human CYP1A2 activity was not affected by nicotine (Hukkanen et al, 2011), which suggests that the pattern, similar to that observed upon smoking cessation, resulted from the absence of inducers such as PAHs in the THS 2.2 aerosol.

Table 2. Changes in CYP1A2 activity in 5-day clinical studies in Japanese and US populations (full analysis set population)

Study	Relative change vs. baseline (%) Mean (SD) [1]			Change vs. reference (%) LS mean [95% CI] [1]	
	THS	CS	SA	THS:CS	THS:SA
ZRHR-REXC-03-EU (Day 5)	−16.5 (18.0)	12.7 (15.7)	−14.9 (15.8)	−33.6 [−40.6; −26.6]	−2.0 [−9.1; 5.1]
ZRHR-REXC-04-JP (Day 5)	−27.4 (14.1)	−1.0 (15.6)	−30.5 (14.8)	−21.7 [−25.5; −17.8]	2.3 [−1.6; 6.2]

CI, confidence interval; CS, cigarette smoke; SA, smoking abstinence; LS, least-squares; SD, standard deviation; THS: Tobacco heating system.
[1] Numbers were rounded to one decimal place.
[Source: Clinical Study Report ZRHR-REXC-03-EU, Tables 66 and 67; and ZRHR-REXC-04-JP, Tables 63 and 64.]

Table 3. Changes in CYP1A2 activity in 3-month clinical studies in Japanese and US populations (full analysis set population)

Study	Relative change vs. baseline (%) Mean (SD) [1]			Ratio of change vs. reference (%) LS mean [95% CI] [1]	
	THS	CS	SA	THS:CS	THS:SA
ZRHM-REXA-07-JP (Day 5)	−21.6 (15.3)	9.7 (23.2)	−23.2 (16.9)	72.1 [67.3; 77.3]	101.8 [94.9; 109.3]
ZRHM-REXA-07-JP (Day 90)	−19.0 (26.7)	15.4 (39.3)	−15.9 (21.5)	70.4 [63.0; 78.7]	93.4 [83.4; 104.6]
ZRHM-REXA-08-US (Day 5)	−33.3 (17.0)	3.2 (13.0)	−29.1 (15.6)	63.0 [58.2; 68.3]	98.4 [90.4; 107.1]
ZRHM-REXA-08-US (Day 90)	−31.7 (27.3)	−13.5 (19.6)	−19.2 (23.7)	77.1 [66.0; 90.0]	84.2 [71.8; 98.9]

CI, confidence interval; LS, least-squares; SD, standard deviation.
[1] Numbers were rounded to one decimal place.
[Source: Clinical Study Report ZRHM-REXA-07-JP, Tables 15.2.4.24.2 and 15.2.4.23.2; and ZRHM-REXA-08-US, Tables 15.2.4.23.2 and 15.2.4.24.2.]

4.3.2 CYP1A1/1B1 activity in organotypic cultures in response to 3R4F or THS 2.2 exposure

A luminescent method was used to measure CYP1A1/1B1 activity in the exposed organotypic cultures. The method is based on luciferin derivatives that, only after conversion by CYPs, react with luciferase to produce light. The amount of light produced is directly proportional to the CYP activity. The combined CYP1A1 and CYP1B1 activity was measured in organotypic tissues by adding luminogenic CYP-Glo luciferin 6′-chloroethyl ether (luciferin-CEE), which is a substrate for both CYP1A1 and CYP1B1, to the basolateral medium 24 hours prior to sample collection. The luciferin product of the CYP reaction was detected after 30 min incubation with detection reagent using a luminescence reader. 2,3,7,8-tetrachlorodibenzo-p-dioxin (TCDD) was used as the positive control to which the 3R4F and THS 2.2-responses were normalized.

In bronchial cultures, the CYP1A1/1B1 activity levels following 3R4F CS were higher than the air control, despite high variability within the group. The CYP1A1/1B1 activity levels in the THS 2.2 aerosol-exposed bronchial cultures were comparable to the air control. In nasal cultures, at the comparable nicotine concentrations (0.13–0.15 mg nicotine/l), the CYP1A1/1B1 activity levels in THS 2.2 aerosol-exposed cultures were lower than those in 3R4F-exposed cultures. In buccal cultures, both 3R4F CS and THS 2.2 aerosol at nicotine concentrations less than 1 mg/l did not substantially influence the CYP1A1/1B1 activity levels (Figure 6C). The CYP1A1/1B1 activity levels in bronchial and nasal cultures following exposure to THS 2.2 aerosol were lower than those following exposure to 3R4F CS, at the comparable nicotine concentrations (at 48 h post-exposure) (Figure 6A and Figure 6B). However, CYP1A1/1B1 activity levels in the buccal cultures were not altered following 3R4F CS, but increased dose-dependently following THS 2.2 aerosol (Figure 6C). The different CYP activity levels suggest that the

expression and activity of CYP1A1/1B1 are regulated differently in different types of epithelial cells.

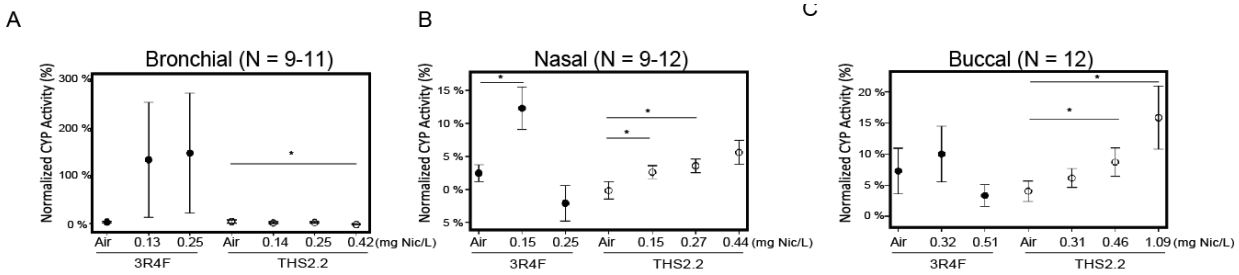


Figure 6. CYP1A1/CYP1B1 activity in organotypic tissue cultures following exposure to 3R4F and THS 2.2.

The combined CYP1A1/1B1 activity level was measured 24, 48, and 72 h after bronchial (A), nasal (B), or buccal (C) organotypic tissue cultures were exposed to 3R4F CS or THS 2.2 aerosol at the indicated nicotine concentrations (mg/l) for 28 min. Data are presented as the mean ± SEM (N = 3–12, from five experimental repetitions with three exposure runs/repetitions) of the normalized activity relative to the positive control (TCDD-treated culture was considered as 100% induction). ★ indicates a significant difference compared with the corresponding air controls (p-values <0.05).

4.4 Activation of the xenobiotic metabolism network in response to 3R4F or THS2.2 exposure

4.4.1 Description of the xenobiotic metabolism network model

The xenobiotic metabolism network model was initially published as part of the biological network model describing various stress responses in lung cells (Schlage et al, 2011) and further refined to better reflect the comprehensive processes in lung tissue (Iskandar et al, 2013). The model is based on the Biological Expression Language (BEL), which was recently released to the life sciences community (http://www.openbel.org). BEL is a structured language that represents scientific findings by capturing causal and correlative relationships between biological entities in computable statements that are composed using functions and entity definitions expressed with a defined ontology (e.g., HGNC, see www.genenames.org).

A browsable view of the recent network models is available at bionet.sbvimprover.com (The sbv Improver project team et al., 2013) and in the Causal Biological Networks database (http://causalbionet.com) (Boué et al, 2015). In the xenobiotic metabolism network model, the central node is the transcriptional activity of aryl hydrocarbon receptor (AHR) (Figure 7). AHR is expressed in most tissues and mediates the effects of dioxins, dioxin-like compounds, and benzo[*a*]pyrene. Dormant AHR resides in the cytoplasm bound to a chaperone complex (Hsp90/XAP2/p23). When activated by xenobiotic compounds, AHR translocates to the nucleus, where heat shock protein Hsp90 is exchanged for the AHR nuclear translocator, ARNT. The heterodimer can then regulate the expression of several target genes, including CYP1A1 and CYP1B1 (Fujii-Kuriyama & Mimura, 2005; Sagredo et al, 2006).

The network contains various biological entities (backbone nodes) that are designed to facilitate the interpretation of numerous gene expression changes and illustrate the fundamental paradigm shift from forward to backward reasoning. The model considers the changes in gene expression to be a consequence of the upstream biological entities

embedded in the backbone nodes (the functional layer). Using backward reasoning, we have developed the network perturbation amplitude (NPA) algorithm that provides a quantification of the backbone nodes, referred to as the "differential network backbone value"(Martin et al, 2014). For instance, the transcriptional activity of AHR is predicted by fold changes in several downstream genes. In other words, the NPA approach provides differential network backbone values that can serve as the basis for network perturbation quantification and a mechanistic explanation.

Figure 7 shows a graphical representation of the backbone of the xenobiotic metabolism network model as well as the scoring principle to assess the perturbation of this network based on predictions from transcriptomics data.

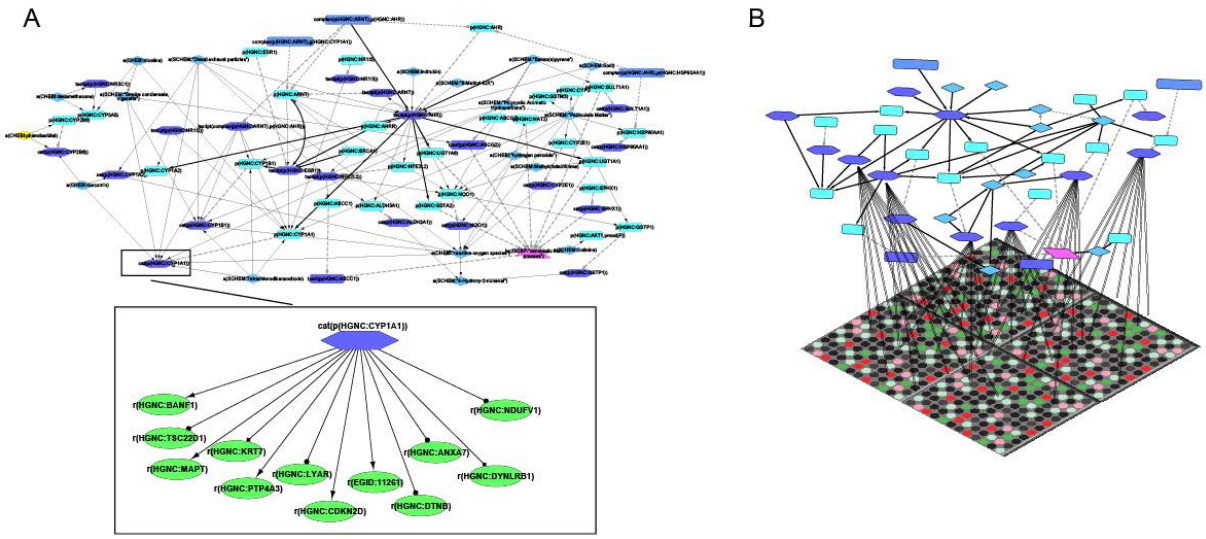


Figure 7. Structure of the xenobiotic metabolism network model and the principle of scoring the network model with transcriptomics data.

A) A large amount of available literature knowledge is harnessed to build causal biological network models that represent biological processes in an easily digestible form. B) The network model also contains a measurable layer, which is represented as mRNA abundances depicting gene expression regulation by molecules present in the model backbone.

4.4.2 Perturbation of the xenobiotic metabolism network model in response to CS and THS 2.2 exposure in rodent lung

The degree of impact of 3R4F CS and THS 2.2 aerosol exposure is reflected by the NPA score. The xenobiotic metabolism network was perturbed only in the lung of ApoE-/- mice exposed to 3R4F, and the impact was greatest at the 8-month time point. No statistically significant perturbation was observed in any of the mouse groups exposed to THS 2.2 or in the groups exposed to 3R4F for 2 months followed by cessation or switching to THS 2.2 (Figure 8A). The nose-only 3R4F exposure of rats also resulted in a significant impact on xenobiotic metabolism, with higher impact observed in female rats and a dose-response impact in the lung of male rats. The impact on xenobiotic metabolism was also observed in the recovery group of females, as well as the males at the highest 3R4F concentration. In contrast to the chronic mouse inhalation studies, the

subchronic rat inhalation studies demonstrated a dose-dependent impact on the xenobiotic metabolism in the female rat lung in response to exposure (Figure 8B). Figure 8C includes the MIS 3R4F and THS 2.2M products and shows that they had no additional impact on xenobiotic metabolism network compared with the impact observed for the regular products.

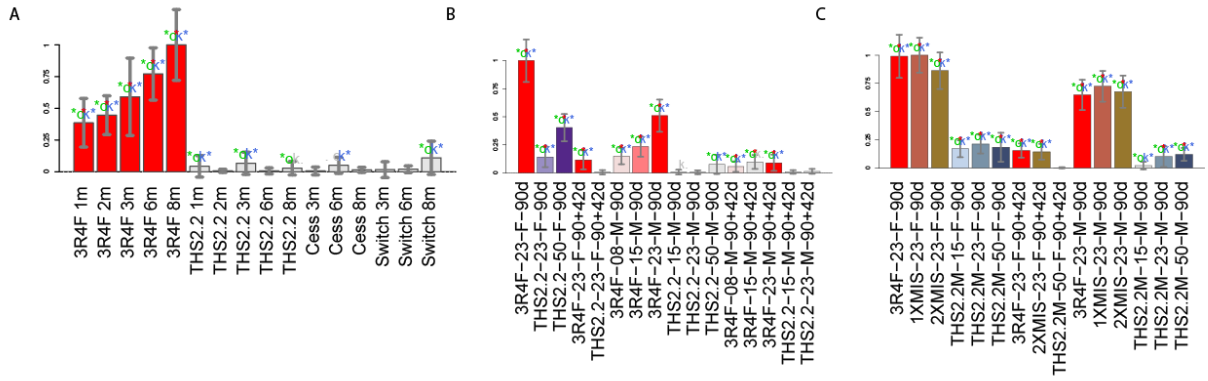


Figure 8. Perturbation of the xenobiotic metabolism network in rodent lungs in response to 3R4F or THS 2.2 exposure.

Gene expression values from CS- or aerosol-treated samples were compared with the gene expression values from the control samples, and the differences were scored against the xenobiotic network model. NPA scores are shown with their confidence interval accounting for experimental variation. The red star indicates NPA scores that are statistically different from 0. Companion statistics that inform on the specificity of the NPA score with respect to the network structure are shown as *O and K* when the p-values are below the significance level of 0.05 (green and blue respectively), and by O and K when the corresponding p-values are between 0.05 and 0.1 (grey). A) ApoE-/- mice switching study. The lanes are labeled with the product (3R4F or THS 2.2) and the time points are indicated after the exposure group. B) OECD THS 2.2 and C) OECD THS 2.2M TG413 studies. In B) and C), the lanes are labeled as [product (3R4F or THS 2.2)-nicotine concentration (mg/l)-sex (F, female; M, male)-exposure time point (90d, 90 days; 90+42d, 90 days of exposure with 42 day recovery)]. MIS, menthol in smoke of 3R4F.

4.4.3 Perturbation of the xenobiotic metabolism network model in response to CS or THS 2.2 exposure in rodent nasal epithelium

The xenobiotic metabolism network perturbation increased with time in the nasal epithelium of mice exposed to 3R4F, and a small impact was observed in response to THS 2.2 exposure at the 6-month time point. A small impact was also observed at the 6- and 8-month time points in the groups that were first exposed to 3R4F for 2 months and then switched to THS 2.2 (Figure 9A). In contrast to the results for rat lung, xenobiotic metabolism in the nasal epithelium of female rats was less impacted by exposure to 3R4F and THS 2.2 (Figure 9B). However, similar to the results for rat lung, the response to THS 2.2 and THS 2.2M resulted in a much smaller impact than 3R4F on xenobiotic metabolism in the rat nasal epithelium (Figure 9B and Figure 9C).

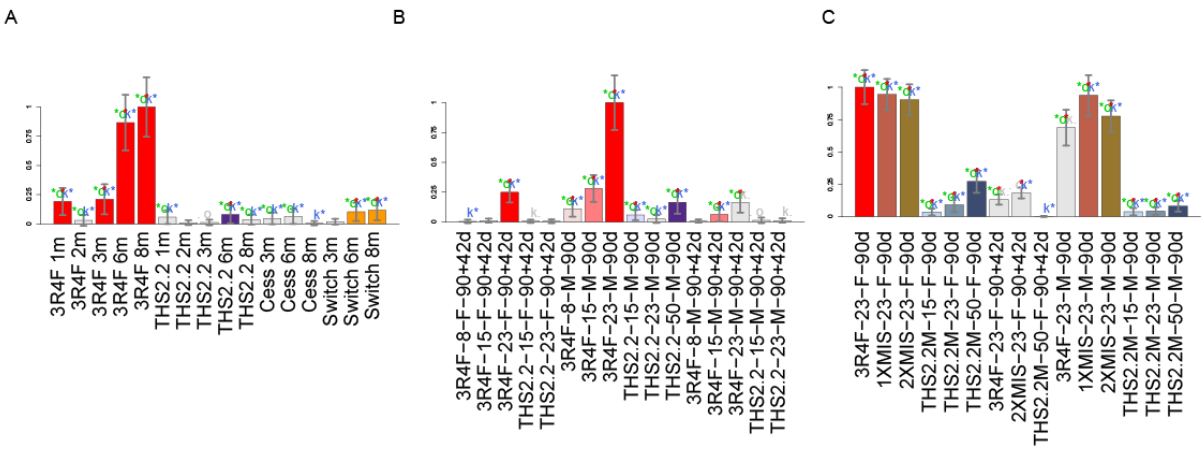


Figure 9. Perturbation of the xenobiotic metabolism network in rodent nasal epithelium in response to 3R4F or THS 2.2 exposure.

Gene expression values from CS- or aerosol-treated samples were compared with the gene expression values from the control samples, and the differences were scored against the xenobiotic network model. NPA scores are shown with their confidence interval accounting for experimental variation. The red star indicates NPA scores that are statistically different from 0. Companion statistics that inform on the specificity of the NPA score with respect to the network structure are shown as *O and K* when the p-values are below the significance level of 0.05 (green and blue respectively), and by O and K when the corresponding p-values are between 0.05 and 0.1 (grey). A) ApoE-/- mice switching study. The lanes are labeled with the product (3R4F or THS 2.2) and the time points are indicated after the exposure group. B) OECD THS 2.2 and C) OECD THS 2.2M TG413 studies. In B) and C), the lanes are labeled as [product (3R4F or THS 2.2)-nicotine concentration (mg/l)-sex (F, female; M, male)-exposure time point (90d, 90 days; 90+42d, 90 days of exposure with 42 day recovery)]. MIS, menthol in smoke of 3R4F.

4.4.4 Perturbation of the xenobiotic metabolism network model in response to CS or THS 2.2 exposure in organotypic tissue cultures

Transcriptomics data from the epithelial cultures following exposure were obtained at 4, 24, 48, and 72 h post-exposure time points. The xenobiotic metabolism network model was used to infer the biological impact of THS 2.2 aerosol and 3R4F CS exposures. While the exposure concentrations varied for the three tissue types (bronchial, nasal, and buccal), the trend in the xenobiotic metabolism response was similar in all three organotypic cultures. At the comparable nicotine concentrations, the NPA score was higher for the 3R4F-exposed cultures compared with THS 2.2-exposed cultures across most post-exposure time points, with the exception being the high THS 2.2 concentrations at 4 h post-exposure in the bronchial and nasal cultures (Figure 10A, Figure 10B, and Figure 10C). The exposure to THS 2.2 at the higher nicotine concentrations resulted in a considerable but transient impact on the xenobiotic metabolism network at the 4 h post-exposure time point, which was not detected in the cultures harvested at the later post-exposure time points.

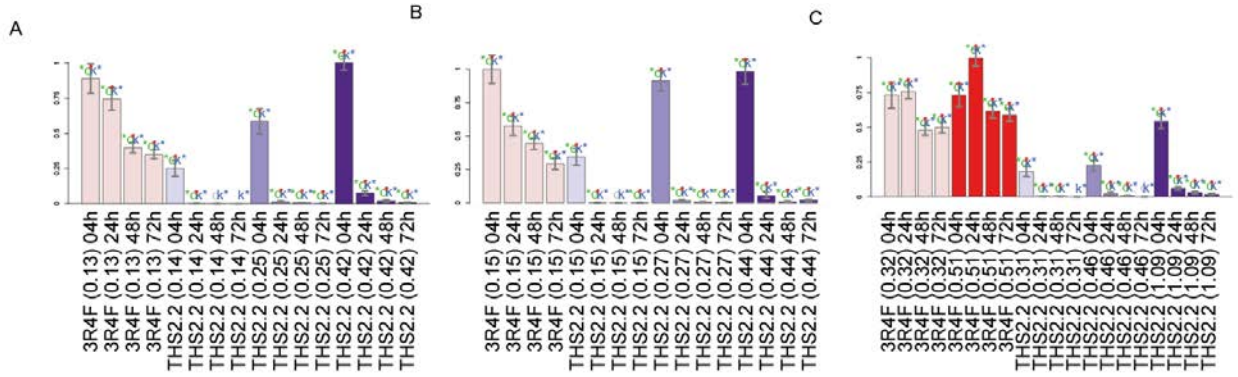


Figure 10. Perturbation of the xenobiotic metabolism network in organotypic tissue cultures in response to CS or THS 2.2 exposure.

A) Bronchial (B) nasal, and C) buccal epithelia. Gene expression values from CS- or aerosol-treated samples were compared with the gene expression values from the control samples, and the differences were scored against the xenobiotic network model. NPA scores at each time point are shown with their confidence interval accounting for experimental variation. The red star indicates NPA scores that are statistically different from 0. Companion statistics that inform on the specificity of the NPA score with respect to the network structure are shown as *O and K* when the p-values are below the significance level of 0.05 (green and blue respectively), and by O and K when the corresponding p-values are between 0.05 and 0.1 (grey). The lanes are labeled with the products (3R4F or THS 2.2) followed by the nicotine concentration (mg/l in parenthesis) and the post-exposure time point.

4.5 Translation of the xenobiotic metabolism response between different experimental systems

The NPA approach and the correlation of the differential network backbone values in the xenobiotic metabolism network model between different datasets can be used to assess the comparability of exposure response in different experimental systems. We have shown previously that quantification of the perturbation of the xenobiotic network model using the NPA approach could be applied not only to compare the responses observed from datasets generated from *in vivo* samples and *in vitro* organotypic models but also to compare the responses from bronchial epithelium and its surrogate nasal epithelium (Iskandar et al, 2013). Below, we have extended these analyses to the data from the comprehensive *in vivo* and *in vitro* studies that assessed the impact of 3R4F and THS 2.2 on xenobiotic metabolism in respiratory tissues.

4.5.1 Response of xenobiotic metabolism to THS 2.2 in pre-clinical models compared with in human studies

To determine the relevance of the pre-clinical models used to assess THS 2.2, the data from different pre-clinical models were compared with data from human bronchial brushings in the context of the xenobiotic metabolism network model. For these comparisons, two public datasets from smoker and nonsmoker bronchial brushings, GSE7895 and GSE19667, were used.

Relatively poor correlation was observed in the differential network backbone values between lungs of ApoE-/- mice exposed to 3R4F and human bronchial brushings from smokers (Figure 11A). In nasal epithelium, the overall correlation was better at early time points; however, the backbone scores for the network were higher in the human smoker bronchial epithelium than in the lungs of ApoE-/- mice exposed to 3R4F (Figure 11B). When the NPA scores increased with time in the mouse nasal epithelium, the correlation with the human smoker samples decreased.

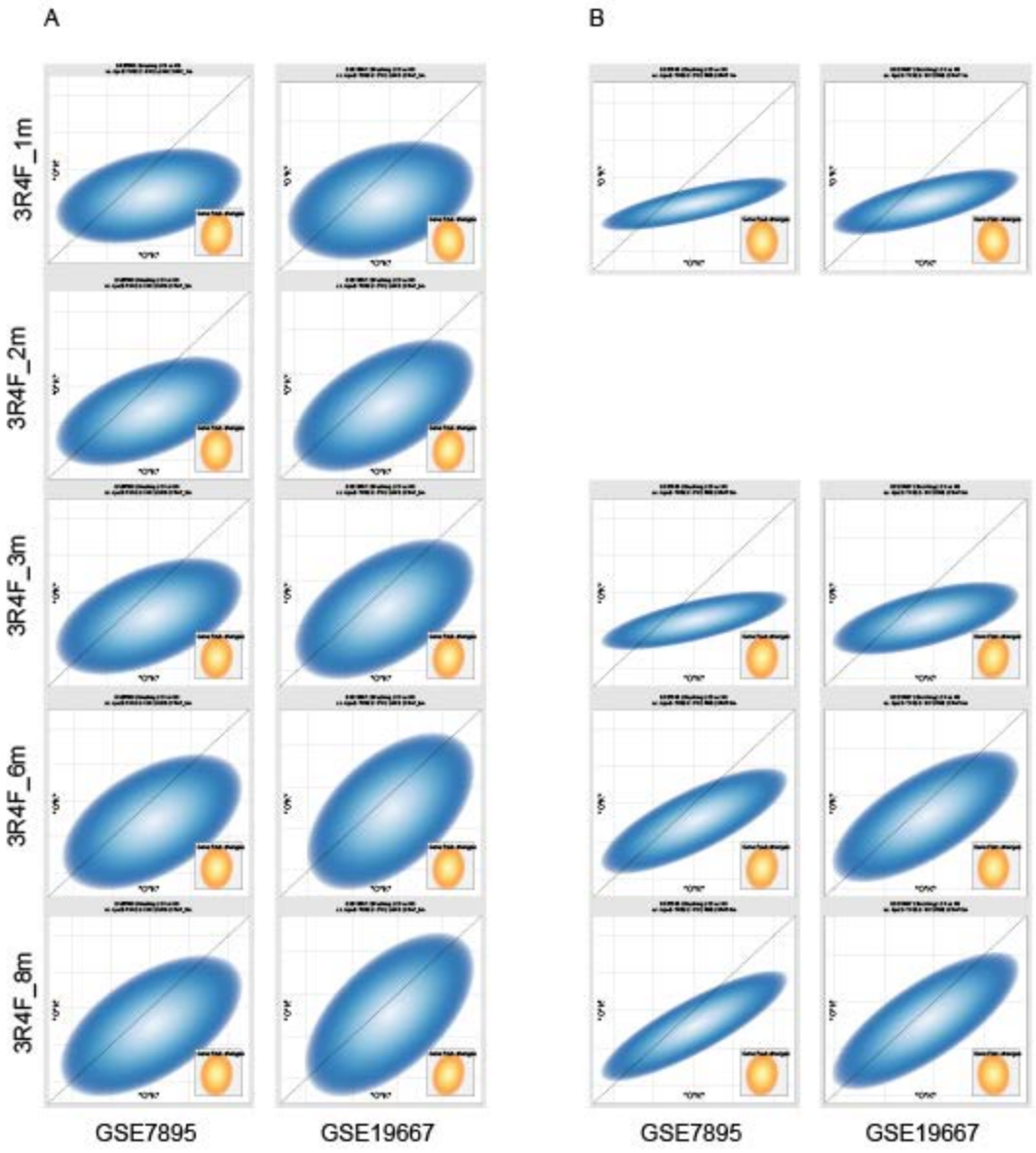


Figure 11. Comparability of the differential network backbone values for the xenobiotic metabolism model from human bronchial brushing datasets and the ApoE-/- mice switching study in response to CS exposure.

A) lung B) nasal epithelium. Gene expression values of CS-treated or human smoker samples were compared with the gene expression values from the control or human nonsmoker samples in the ApoE-/- mice switching study or the Gene Expression Omnibus GSE7895 and GSE19667 datasets, respectively. The differences were scored against the xenobiotic network model. Blue ellipses depict the 95% confidence interval for the cloud of points that represent the differential network backbone values for the two effects compared. The orange ellipses depict the 95% confidence interval for the cloud of points that represent the fold changes for the genes underlying the network backbone. The diagonal lines represent the equality of the differential network backbone values ($y = x$).

The differential network backbone values for the xenobiotic metabolism network model correlated well between lungs of rats exposed to the lowest dose of 3R4F and human smoker bronchial epithelium (Figure 12A). Similar to the ApoE-/- mouse nasal epithelium, the amplitude for the individual backbone values was higher in the rat lung compared with the smoker brushings. Again, when the differential network backbone values increased with nicotine concentration in the rat lung, the correlation with the human samples decreased. The correlation between the nasal epithelium of rats exposed to 3R4F and human smoker bronchial epithelium was poor at all nicotine concentrations (Figure 12B).

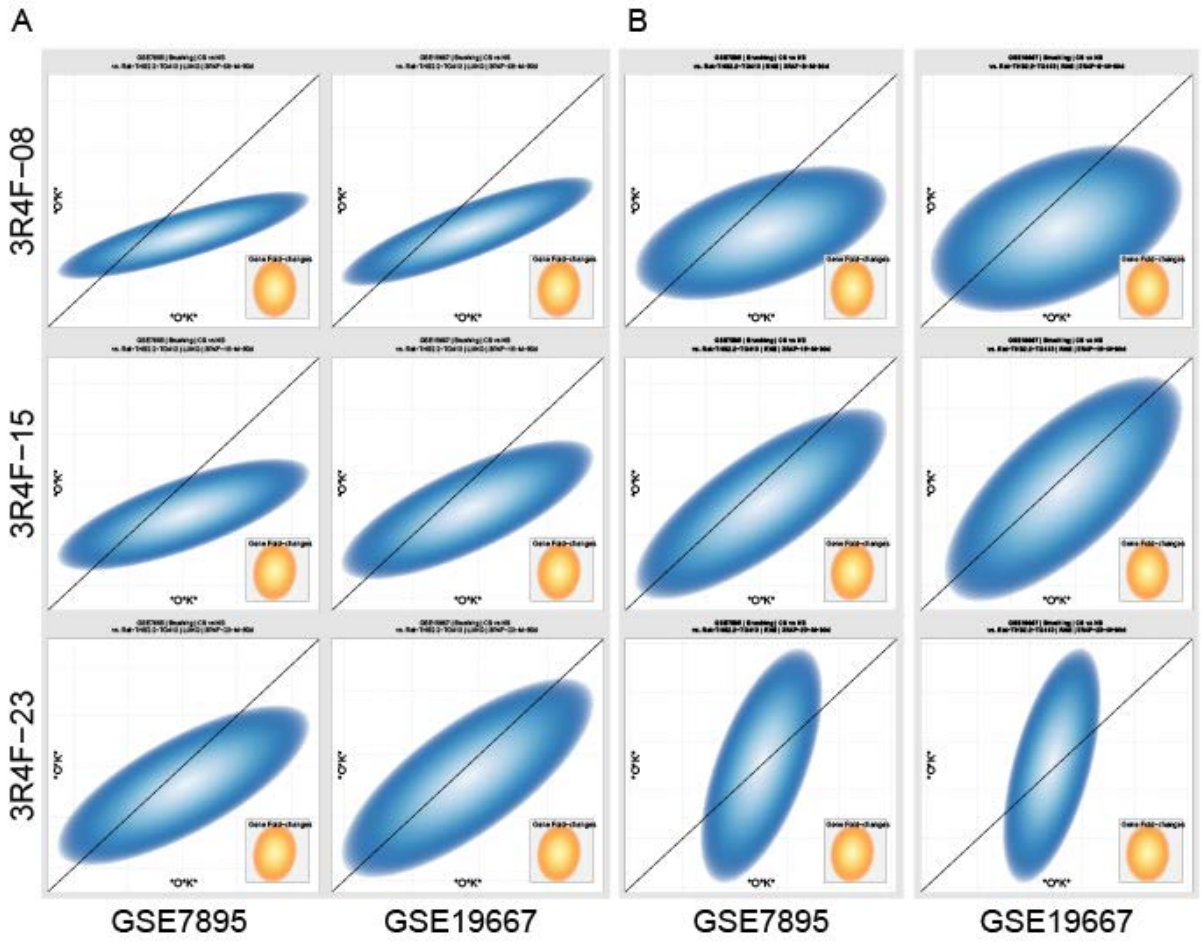


Figure 12. Comparability of the differential network backbone values for the xenobiotic metabolism network between human smoker bronchial brushings and rat respiratory tissues from the OECD THS 2.2 and OECD THS 2.2M TG413 studies.

A) Lung and B) nasal epithelium. Gene expression values of CS-exposed rat lungs or human smoker samples were compared with the gene expression values from the control or human nonsmoker samples in the OECD THS 2.2 and THS 2.2M TG413 studies or the Gene Expression Omnibus GSE7895 and GSE19667 datasets, respectively. The differences were scored against the xenobiotic network model. Blue ellipses depict the 95% confidence interval for the cloud of points that represent the differential network backbone values for the two effects compared. The orange ellipses depict the 95% confidence interval for

the cloud of points that represent fold changes for the genes underlying the network backbone. The diagonal lines represent the equality of the differential network backbone values (y =x). The nicotine concentration (μg/l) is indicated after 3R4F.

Finally, the human smoker bronchial brushings were compared with the organotypic tissue cultures exposed to CS by correlating the differential network backbone scores within the xenobiotic metabolism network. Overall, the correlation between the differential network backbone scores between the two datasets was better than the correlation with the gene level comparison (Figure 13), and the later time points better reflected the magnitude of the scores.

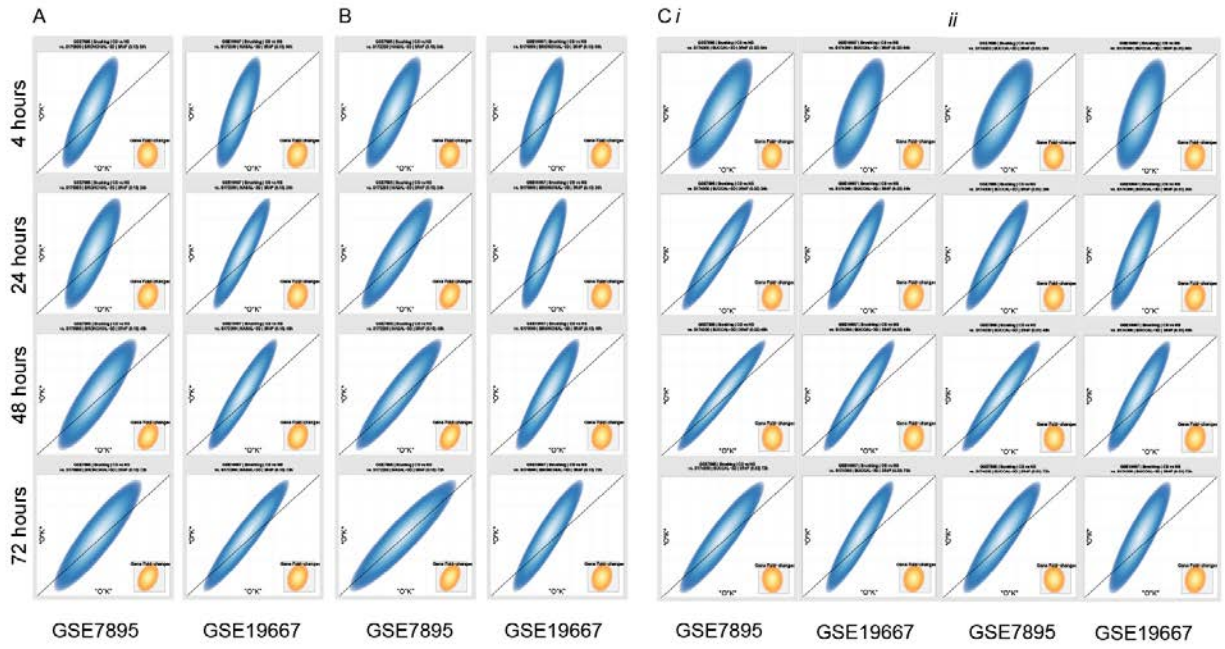


Figure 13. Comparability of the differential network backbone values for the xenobiotic metabolism model between human bronchial brushing datasets and in vitro organotypic cultures in response to smoke exposure.

Gene expression values of CS-treated organotypic tissue cultures or human smoker samples were compared with the gene expression values from the control or human nonsmoker samples in organotypic or the Gene Expression Omnibus GSE7895 and GSE19667 datasets, respectively. The differences were scored against the xenobiotic network model. Blue ellipses depict the 95% confidence interval for the cloud of points that represent the differential network backbone values for the two effects compared. The orange ellipses depict the 95% confidence interval of the cloud of points that represent fold changes for the genes underlying the network backbone. The diagonal lines represent the equality of the differential network backbone values (y = x). A) Bronchial, B) nasal, and C) buccal epithelia; Ci) 032, Cii) 0.5 mg nicotine /1.

4.5.2 Comparability of 3R4F CS and THS 2.2 aerosol exposure in the context of the xenobiotic metabolism network

An important aspect in harm reduction assessment is to compare the conventional cigarette 3R4F with the THS 2.2 in a relevant biological context. Where possible, the xenobiotic network model was used to compare the different products. The only sample in the ApoE-/- mouse study that showed perturbation of the xenobiotic metabolism network by THS 2.2 exposure was the nasal epithelium at the 6-month time point. While good correlation in the differential network backbone values was observed between the nasal epithelium of mice exposed to 3R4F for 6 or 8 months and those exposed to THS 2.2 for 6 months, the differential network backbone values were much lower for the nasal epithelium of ApoE-/- mice exposed to THS 2.2 (Figure 14).

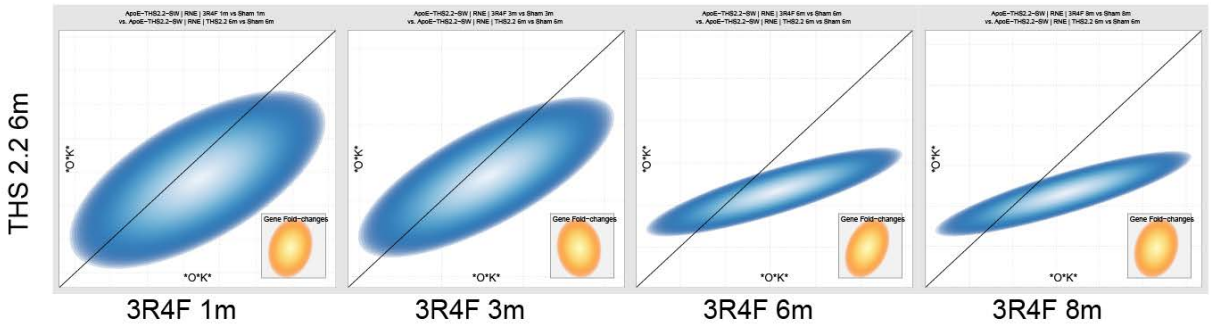


Figure 14. Comparability of the differential network backbone values for the xenobiotic metabolism model in nasal epithelium of ApoE-/- mice exposed to 3R4F or THS 2.2.

Gene expression values of CS- or aerosol-treated samples were compared with the gene expression values from the control samples in the ApoE-/-mice switching study. Blue ellipses depict the 95% confidence interval for the cloud of points that represent the differential network backbone values for the two effects compared. The orange ellipses depict the 95% confidence interval for the cloud of points that represent fold changes for the genes underlying the network backbone. The diagonal lines represent the equality of the differential network backbone values (y = x).

The extensive design of the OECD TG413 studies allowed the comparison of both 3R4F and MIS 3R4F with THS 2.2 and THS 2.2M. The correlation in the backbone scores was good between the lungs of rats exposed to 3R4F and THS 2.2 for 6 months; however, the differential network backbone values were much lower in the lungs of rats exposed to THS 2.2 and the correlation decreased with increasing THS 2.2 nicotine concentrations (Figure 15).

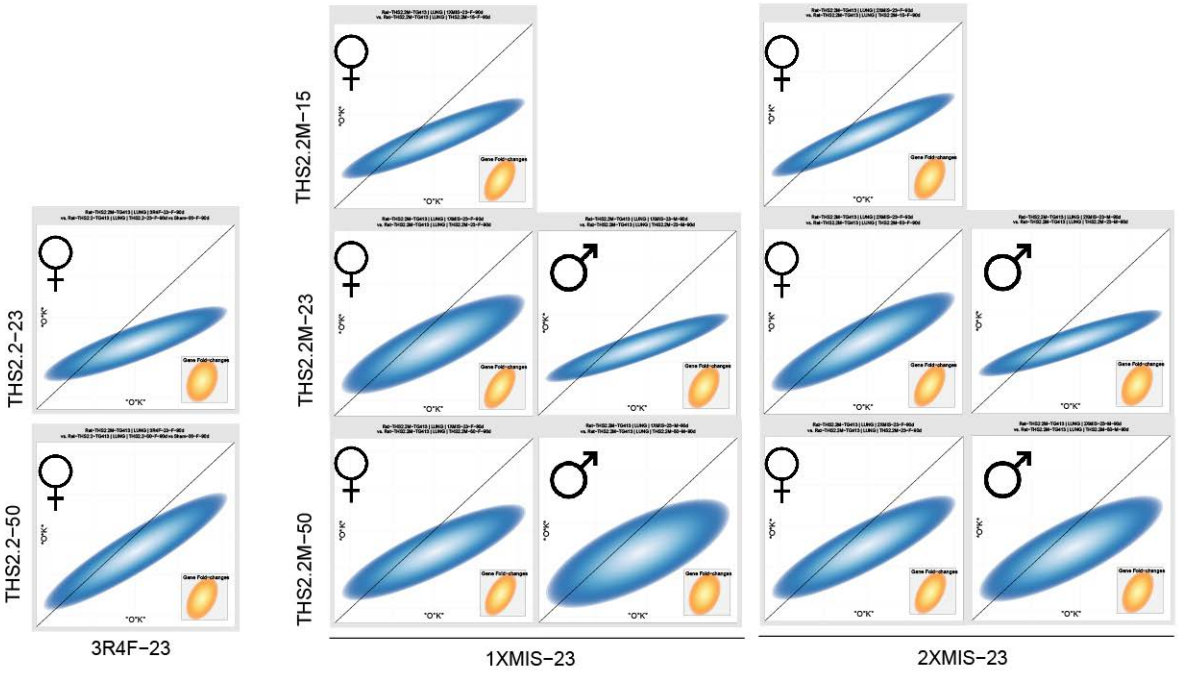


Figure 15. Comparability of the differential network backbone values for the xenobiotic metabolism model between lungs of rats exposed to 3R4F, 1×MIS, or 2×MIS and lungs of rats exposed to THS 2.2 or THS 2.2M for 90 days.

Gene expression values of CS- or aerosol-treated samples were compared with the gene expression values from the control samples in the OECD THS 2.2M TG413 study. The differences were scored against the xenobiotic network model. Blue ellipses depict the 95% confidence interval for the cloud of points that represent the differential network backbone values for the two effects compared. The orange ellipses depict the 95% confidence interval or the cloud of points that represent fold changes for the genes underlying the network backbone. The diagonal lines represent the equality of the differential network backbone values (y = x). The nicotine concentration (µg/l) is indicated after each product. MIS, menthol in smoke of 3R4F.

The correlations of the differential network backbone scores for the organotypic tissue cultures in response to 3R4F or THS 2.2 exposure are shown in Figure 16. The 4 hour post-exposure time point was chosen for the comparisons because the impact on the network was maximal at this time point. The correlation between 3R4F and THS 2.2 in all three organotypic tissue models was remarkably high; however, a higher nicotine concentration in the THS 2.2 aerosol compared with CS was required for the same impact, which might be a result of the different structure and sensitivity of the three organotypic tissues, particularly the relatively thick and robust buccal epithelium.

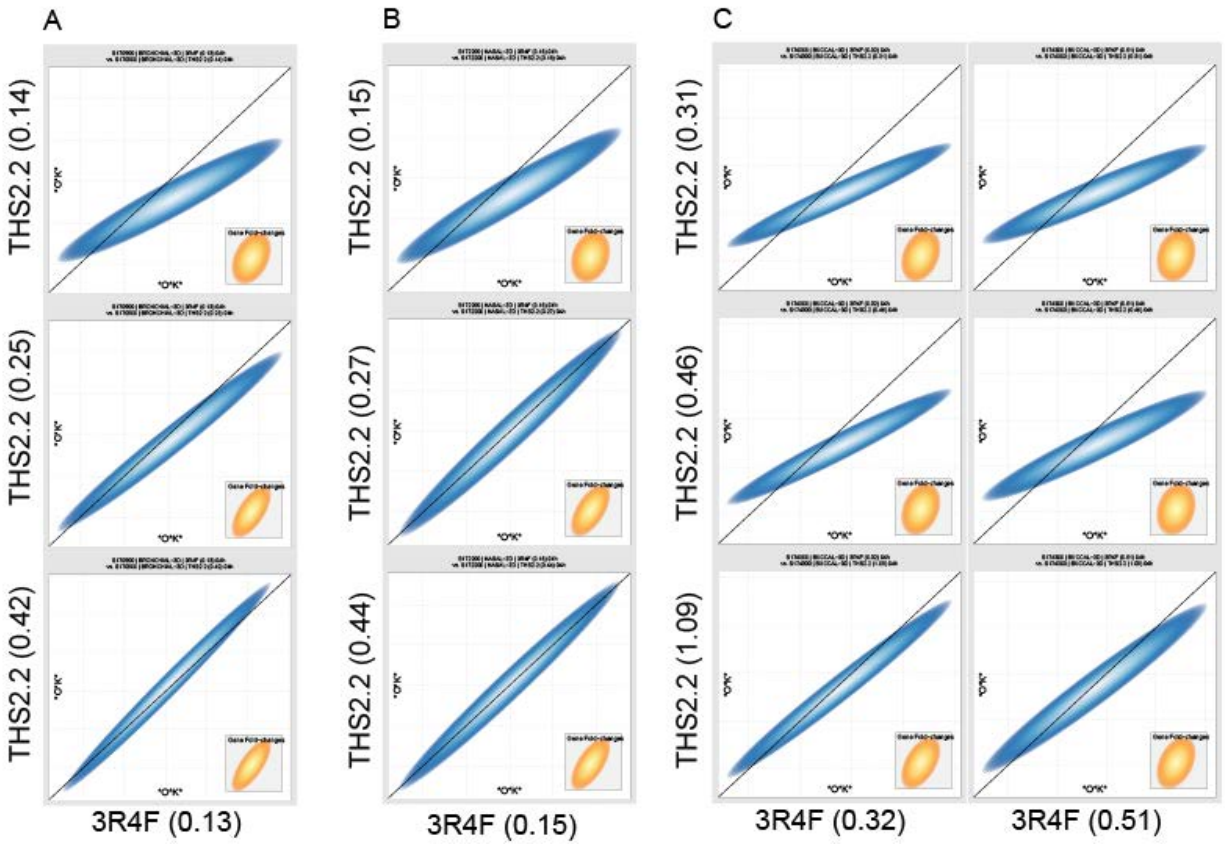


Figure 16. Comparability of the differential network backbone values for the xenobiotic metabolism model in organotypic cultures exposed to 3R4F or THS 2.2.

Gene expression values of CS- or aerosol-treated samples were compared with the gene expression values from the control samples in the organotypic exposure studies. Blue ellipses depict the 95% confidence interval for the cloud of points that represent the differential network backbone values for the two effects compared. The orange ellipses depict the 95% confidence interval for the cloud of points that represent fold changes for the genes underlying the network backbone. The diagonal lines represent the equality of the differential network backbone values (y = x). The nicotine concentration (µg/l) is indicated after each product. A) Bronchial, B) nasal, and C) buccal epithelia.

5 CONCLUSIONS

Our analyses of the differential expression patterns of the genes encoding XMEs and transporters relevant to the respiratory tract demonstrated that exposure to THS 2.2 aerosol had a smaller impact than exposure to the smoke from the combustible reference cigarette 3R4F in all pre-clinical models tested. In the context of the biological network model that captures the xenobiotic metabolism response in the respiratory tract, we observed an overall weaker perturbation of the model by THS 2.2 aerosol compared with CS at nicotine-matched exposure concentrations. In the organotypic tissue culture models, the response to THS 2.2 aerosol exposure was transient and limited to the 4-hour time point, whereas the CS response declined slowly and remained elevated throughout the 72 hours post-exposure. Taken together, these results demonstrate an overall reduced impact on xenobiotic metabolism for exposure to THS 2.2/THS 2.2M aerosols compared with CS in nonclinical *in vitro* and *in vivo* models. Moreover, the responses from the nonclinical exposure studies were compared with results obtained from human smokers on a qualitative and quantitative basis using the network modeling approach, and a high degree of translational correlation was shown between the systems.

6 REFERENCES

Anttila S, Hirvonen A, Vainio H, Husgafvel-Pursiainen K, Hayes JD, Ketterer B (1993) Immunohistochemical localization of glutathione S-transferases in human lung. *Cancer Research* **53:** 5643-5648

Arlt VM, Krais AM, Godschalk RW, Riffo-Vasquez Y, Mrizova I, Roufosse CA, Corbin C, Shi Q, Frei E, Stiborova M (2015) Pulmonary inflammation impacts on CYP1A1-mediated respiratory tract DNA damage induced by the carcinogenic air pollutant benzo [a] pyrene. *Toxicological Sciences***:** kfv086

Balendiran GK, Martin H-J, El-Hawari Y, Maser E (2009) Cancer biomarker AKR1B10 and carbonyl metabolism. *Chemico-biological interactions* **178:** 134-137

Bartsch H, Rojas M, Alexandrov K, Camus A-M, Castegnaro M, Malaveille C, Anttila S, Husgafvel-Pursiainen K, Hietanen E, Vainio H (1995) Metabolic polymorphism affecting DNA binding and excretion of carcinogens in humans. *Pharmacogenetics and Genomics* **5:** S84-S90

Baxter A, Thain S, Banerjee A, Haswell L, Parmar A, Phillips G, Minet E (2015) Targeted omics analyses, and metabolic enzyme activity assays demonstrate maintenance of key mucociliary characteristics in long term cultures of reconstituted human airway epithelia. *Toxicology in Vitro* **29:** 864-875

Bebenek IG, Solaimani P, Bui P, Hankinson O (2012) CYP2S1 is negatively regulated by corticosteroids in human cell lines. *Toxicology letters* **209:** 30-34

Benowitz NL, Hukkanen J, Jacob III P (2009) Nicotine chemistry, metabolism, kinetics and biomarkers. *Handb Exp Pharmacol* **192:** 29-60

Berg T, Hegelund Myrbäck T, Olsson M, Seidegård J, Werkström V, Zhou XH, Grunewald J, Gustavsson L, Nord M (2014) Gene expression analysis of membrane transporters and drug-metabolizing enzymes in the lung of healthy and COPD subjects. *Pharmacology research & perspectives* **2**

Bernauer U, Heinrich-Hirsch B, Tönnies M, Peter-Matthias W, Gundert-Remy U (2006) Characterisation of the xenobiotic-metabolizing Cytochrome P450 expression pattern in human lung tissue by immunochemical and activity determination. *Toxicology letters* **164:** 278-288

Bieche I, Narjoz C, Asselah T, Vacher S, Marcellin P, Lidereau R, Beaune P, de Waziers I (2007) Reverse transcriptase-PCR quantification of mRNA levels from cytochrome (CYP) 1, CYP2 and CYP3 families in 22 different human tissues. *Pharmacogenetics and genomics* **17:** 731-742

Boué S, Talikka M, Westra JW, Hayes W, Di Fabio A, Park J, Schlage WK, Sewer A, Fields B, Ansari S (2015) Causal biological network database: a comprehensive platform of causal biological network models focused on the pulmonary and vascular systems. *Database* **2015:** bav030

Bréchot J-M, Hurbain I, Fajac A, Daty N, Bernaudin J-F (1998) Different pattern of MRP localization in ciliated and basal cells from human bronchial epithelium. *Journal of Histochemistry & Cytochemistry* **46:** 513-517

Bushey RT, Chen G, Blevins-Primeau AS, Krzeminski J, Amin S, Lazarus P (2011) Characterization of UDP-glucuronosyltransferase 2A1 (UGT2A1) variants and their potential role in tobacco carcinogenesis. *Pharmacogenetics and genomics* **21:** 55

Bushey RT, Dluzen DF, Lazarus P (2013) Importance of UDP-glucuronosyltransferases 2A2 and 2A3 in tobacco carcinogen metabolism. *Drug Metabolism and Disposition* **41:** 170-179

Cantrell E, Warr G, Busbee D, Martin R (1973) Induction of aryl hydrocarbon hydroxylase in human pulmonary alveolar macrophages by cigarette smoking. *Journal of Clinical Investigation* **52:** 1881

Castell JV, Donato MT, Gomez-Lechon MJ (2005) Metabolism and bioactivation of toxicants in the lung. The in vitro cellular approach. *Experimental and toxicologic pathology : official journal of the Gesellschaft fur Toxikologische Pathologie* **57 Suppl 1:** 189-204

Chang H, Chang LW, Cheng Y-H, Tsai W-T, Tsai M-X, Lin P (2006) Preferential induction of CYP1A1 and CYP1B1 in CCSP-positive cells. *Toxicological Sciences* **89:** 205-213

Chen W, Zheng G, Yang S, Ping W, Fu X, Zhang N, Wang DW, Wang J (2014) CYP2J2 and EETs protect against oxidative stress and apoptosis in vivo and in vitro following lung ischemia/reperfusion. *Cellular Physiology and Biochemistry* **33:** 1663-1680

Chiang H-c, Wang C-K, Tsou T-C (2012) Differential distribution of CYP2A6 and CYP2A13 in the human respiratory tract. *Respiration* **84:** 319-326

Choudhary D, Jansson I, Schenkman J, Sarfarazi M, Stoilov I (2003) Comparative expression profiling of 40 mouse cytochrome P450 genes in embryonic and adult tissues. *Archives of Biochemistry and Biophysics* **414:** 91-100

Cohen GM (1990) Pulmonary metabolism of foreign compounds: its role in metabolic activation. *Environmental health perspectives* **85:** 31

Croom E (2012) 3 Metabolism of Xenobiotics of Human Environments. *Progress in molecular biology and translational science* **112:** 31

Dahl A, Lewis J (1993) Respiratory tract uptake of inhalants and metabolism of xenobiotics. *Annual review of pharmacology and toxicology* **33:** 383-407

Dairou J, Petit E, Ragunathan N, Baeza-Squiban A, Marano F, Dupret J-M, Rodrigues-Lima F (2009) Arylamine N-acetyltransferase activity in bronchial epithelial cells and its inhibition by cellular oxidants. *Toxicology and applied pharmacology* **236:** 366-371

DeVore NM, Scott EE (2012) Nicotine and 4-(methylnitrosamino)-1-(3-pyridyl)-1-butanone binding and access channel in human cytochrome P450 2A6 and 2A13 enzymes. *Journal of Biological Chemistry* **287:** 26576-26585

Ding X, Kaminsky LS (2003) HUMAN EXTRAHEPATIC CYTOCHROMES P450: Function in Xenobiotic Metabolism and Tissue-Selective Chemical Toxicity in the Respiratory and Gastrointestinal Tracts*. *Annual review of pharmacology and toxicology* **43:** 149-173

Faber MS, Fuhr U (2004) Time response of cytochrome P450 1A2 activity on cessation of heavy smoking. *Clinical Pharmacology & Therapeutics* **76:** 178-184

Foth H (1995) Role of the lung in accumulation and metabolism of xenobiotic compounds-implications for chemically induced toxicity. *CRC Critical Reviews in Toxicology* **25:** 165-205

Foth H, Looschen H, Neurath H, Kahl GF (1991) Nicotine metabolism in isolated perfused lung and liver of phenobarbital-and benzoflavone-treated rats. *Archives of toxicology* **65:** 68-72

Franciosi L, Postma DS, Van Den Berge M, Govorukhina N, Horvatovich PL, Fusetti F, Poolman B, Lodewijk ME, Timens W, Bischoff R (2014) Susceptibility to COPD: differential proteomic profiling after acute smoking. *PloS one* **9:** e102037

Fujii-Kuriyama Y, Mimura J (2005) Molecular mechanisms of AhR functions in the regulation of cytochrome P450 genes. *Biochemical and biophysical research communications* **338:** 311-317

Fukumoto S-i, Yamauchi N, Moriguchi H, Hippo Y, Watanabe A, Shibahara J, Taniguchi H, Ishikawa S, Ito H, Yamamoto S (2005) Overexpression of the Aldo-Keto Reductase Family Protein AKR1B10 Is Highly Correlated with Smokers' Non–Small Cell Lung Carcinomas. *Clinical Cancer Research* **11:** 1776-1785

Gallagher CJ, Muscat JE, Hicks AN, Zheng Y, Dyer A-M, Chase GA, Richie J, Lazarus P (2007) The UDP-glucuronosyltransferase 2B17 gene deletion polymorphism: sex-specific association with urinary 4-(methylnitrosamino)-1-(3-pyridyl)-1-butanol glucuronidation phenotype and risk for lung cancer. *Cancer Epidemiology Biomarkers & Prevention* **16:** 823-828

Garcia-Canton C, Minet E, Anadon A, Meredith C (2013) Metabolic characterization of cell systems used in in vitro toxicology testing: lung cell system BEAS-2B as a working example. *Toxicology in Vitro* **27:** 1719-1727

Gebel S, Gerstmayer B, Bosio A, Haussmann H-J, Van Miert E, Müller T (2004) Gene expression profiling in respiratory tissues from rats exposed to mainstream cigarette smoke. *Carcinogenesis* **25:** 169-178

Gelhaus SL, Gilad O, Hwang W-T, Penning TM, Blair IA (2012) Multidrug resistance protein (MRP) 4 attenuates benzo [a] pyrene-mediated DNA-adduct formation in human bronchoalveolar H358 cells. *Toxicology letters* **209:** 58-66

Gerde P, Muggenburg BA, Scott GG, Lewis JL, Pyon KH, Dahl AR (1998) Local metabolism in lung airways increases the uncertainty of pyrene as a biomarker of polycyclic aromatic hydrocarbon exposure. *Carcinogenesis* **19:** 493-500

Guengerich FP (2000) Metabolism of chemical carcinogens. *Carcinogenesis* **21:** 345-351

Guengerich FP (2003) Cytochromes P450, drugs, and diseases. *Molecular interventions* **3:** 194

Guengerich FP, Shimada T (1998) Activation of procarcinogens by human cytochrome P450 enzymes. *Mutation Research/Fundamental and Molecular Mechanisms of Mutagenesis* **400:** 201-213

Gümüş ZH, Du B, Kacker A, Boyle JO, Bocker JM, Mukherjee P, Subbaramaiah K, Dannenberg AJ, Weinstein H (2008) Effects of tobacco smoke on gene expression and cellular pathways in a cellular model of oral leukoplakia. *Cancer Prevention Research* **1:** 100-111

Gundert-Remy U, Bernauer U, Blömeke B, Döring B, Fabian E, Goebel C, Hessel S, Jäckh C, Lampen A, Oesch F (2014) Extrahepatic metabolism at the body's internal-external interfaces. *Drug metabolism reviews* **46:** 291-324

Hecht SS (1999) Tobacco smoke carcinogens and lung cancer. *Journal of the national cancer institute* **91:** 1194-1210

Hukkanen J, Jacob III P, Peng M, Dempsey D, Benowitz NL (2011) Effect of nicotine on cytochrome P450 1A2 activity. *British journal of clinical pharmacology* **72:** 836-838

Hukkanen J, Pelkonen O, Hakkola J, Raunio H (2002) Expression and regulation of xenobiotic-metabolizing cytochrome P450 (CYP) enzymes in human lung. *Crit Rev Toxicol* **32:** 391-411

Iba MM, Fung J, Pak YW, Thomas PE, Fisher H, Sekowski A, Halladay AK, Wagner GC (1999) Dose-dependent up-regulation of rat pulmonary, renal, and hepatic cytochrome P-450 (CYP) 1A expression by nicotine feeding. *Drug metabolism and disposition* **27:** 977-982

Ishii T, Matsuse T, Igarashi H, Masuda M, Teramoto S, Ouchi Y (2001) Tobacco smoke reduces viability in human lung fibroblasts: protective effect of glutathioneS-transferase P1. *American Journal of Physiology-Lung Cellular and Molecular Physiology* **280:** L1189-L1195

Iskandar AR, Martin F, Talikka M, Schlage WK, Kostadinova R, Mathis C, Hoeng J, Peitsch MC (2013) Systems approaches evaluating the perturbation of xenobiotic metabolism in response to cigarette smoke exposure in nasal and bronchial tissues. *BioMed research international* **2013**

Jang J-H, Bruse S, Liu Y, Duffy V, Zhang C, Oyamada N, Randell S, Matsumoto A, Thompson DC, Lin Y (2014) Aldehyde dehydrogenase 3A1 protects airway epithelial cells from cigarette smoke-induced DNA damage and cytotoxicity. *Free Radical Biology and Medicine* **68:** 80-86

Jiao L, Chang P, Firozi PF, Lai D, Abbruzzese JL, Li D (2007) Polymorphisms of phase II xenobiotic-metabolizing and DNA repair genes and in vitro N-ethyl-N-nitrosourea-induced O 6-ethylguanine levels in human lymphocytes. *Mutation Research/Genetic Toxicology and Environmental Mutagenesis* **627:** 146-157

Jones NR, Lazarus P (2014) UGT2B gene expression analysis in multiple tobacco carcinogen-targeted tissues. *Drug Metabolism and Disposition* **42:** 529-536

Kanehisa M, Goto S, Sato Y, Kawashima M, Furumichi M, Tanabe M (2014) Data, information, knowledge and principle: back to metabolism in KEGG. *Nucleic acids research* **42:** D199-D205

Kondraganti SR, Fernandez-Salguero P, Gonzalez FJ, Ramos KS, Jiang W, Moorthy B (2003) Polycyclic aromatic hydrocarbon-inducible DNA adducts: Evidence by 32P-postlabeling and use of knockout mice for Ah receptor-independent mechanisms of metabolic activation in vivo. *International journal of cancer* **103:** 5-11

Lazarus P, Zheng Y, Runkle EA, Muscat JE, Wiener D (2005) Genotype–phenotype correlation between the polymorphic UGT2B17 gene deletion and NNAL glucuronidation activities in human liver microsomes. *Pharmacogenetics and genomics* **15:** 769-778

Leslie EM, Ito K, Upadhyaya P, Hecht SS, Deeley RG, Cole SP (2001) Transport of the beta -O-glucuronide conjugate of the tobacco-specific carcinogen 4-(methylnitrosamino)-1-(3-pyridyl)-1-butanol (NNAL) by the multidrug resistance protein 1 (MRP1). Requirement for glutathione or a non-sulfur-containing analog. *The Journal of biological chemistry* **276:** 27846-27854

Lo Sasso G, Titz B, Nury C, Boué S, Phillips B, Belcastro V, Schneider T, Dijon S, Baumer K, Peric D (2016) Effects of cigarette smoke, cessation and switching to a candidate modified risk tobacco product on the liver in Apoe−/− mice–a systems toxicology analysis. *Inhalation Toxicology***:** 1-15

Lundgren DH, Hwang S-I, Wu L, Han DK (2010) Role of spectral counting in quantitative proteomics. *Expert review of proteomics* **7:** 39-53

Maertens LA, Upadhyaya P, Hecht SS, Zimmerman CL (2010) Formation and distribution of NNK metabolites in an isolated perfused rat lung. *Drug Metabolism and Disposition* **38:** 752-760

Mahajan MK, Uttamsingh V, Daniels JS, Gan L-S, LeDuc BW, Williams DA (2011) In vitro metabolism of oxymetazoline: evidence for bioactivation to a reactive metabolite. *Drug Metabolism and Disposition* **39:** 693-702

Marchitti SA, Brocker C, Stagos D, Vasiliou V (2008) Non-P450 aldehyde oxidizing enzymes: the aldehyde dehydrogenase superfamily. *Expert opinion on drug metabolism & toxicology* **4:** 697-720

Martin F, Sewer A, Talikka M, Xiang Y, Hoeng J, Peitsch MC (2014) Quantification of biological network perturbations for mechanistic insight and diagnostics using two-layer causal models. *BMC bioinformatics* **15:** 238

Mattammal MB, Lakshmi V, Zenser T, Davis B (1987) Lung prostaglandin H synthase and mixed-function oxidase metabolism of nicotine. *Journal of Pharmacology and Experimental Therapeutics* **242:** 827-832

Mazaki T, Masuda H, Takayama T (2011) Polymorphisms and pancreatic cancer risk: a meta-analysis. *European Journal of Cancer Prevention* **20:** 169-183

Megaraj V, Zhou X, Xie F, Liu Z, Yang W, Ding X (2014) Role of CYP2A13 in the bioactivation and lung tumorigenicity of the tobacco-specific lung procarcinogen 4-(methylnitrosamino)-1-(3-pyridyl)-1-butanone: in vivo studies using a CYP2A13-humanized mouse model. *Carcinogenesis* **35:** 131-137

Modesto JL, Hull A, Angstadt AY, Berg A, Gallagher CJ, Lazarus P, Muscat JE (2015) NNK reduction pathway gene polymorphisms and risk of lung cancer. *Molecular carcinogenesis* **54**

Moorthy B, Chu C, Carlin DJ (2015) Polycyclic Aromatic Hydrocarbons: From Metabolism to Lung Cancer. *Toxicological Sciences* **145:** 5-15

Morita K, Miyazaki H, Saruwatari J, Oniki K, Kumagae N, Tanaka T, Kajiwara A, Otake K, Ogata Y, Arima Y (2015) Combined effects of current-smoking and the aldehyde dehydrogenase 2* 2 allele on the risk of myocardial infarction in Japanese patients. *Toxicology letters* **232:** 221-225

Muto M, Nakane M, Hitomi Y, Yoshida S, Sasaki S, Ohtsu A, Yoshida S, Ebihara S, Esumi H (2002) Association between aldehyde dehydrogenase gene polymorphisms and the phenomenon of field cancerization in patients with head and neck cancer. *Carcinogenesis* **23:** 1759-1766

Myrand S, Sekiguchi K, Man M, Lin X, Tzeng RY, Teng CH, Hee B, Garrett M, Kikkawa H, Lin CY (2008) Pharmacokinetics/Genotype Associations for Major Cytochrome P450 Enzymes in Native and First-and Third-generation Japanese Populations: Comparison With Korean, Chinese, and Caucasian Populations. *Clinical Pharmacology & Therapeutics* **84:** 347-361

Nebert DW, Shi Z, Gálvez-Peralta M, Uno S, Dragin N (2013) Oral benzo [a] pyrene: understanding pharmacokinetics, detoxication, and consequences—Cyp1 knockout mouse lines as a paradigm. *Molecular pharmacology* **84:** 304-313

Newland N, Baxter A, Hewitt K, Minet E (2011) CYP1A1/1B1 and CYP2A6/2A13 activity is conserved in cultures of differentiated primary human tracheobronchial epithelial cells. *Toxicology In Vitro* **25:** 922-929

Oesch-Bartlomowicz B, Oesch F, Testa B, van de Waterbeemd H (2007) Mechanisms of toxification and detoxification that challenge drug candidates and drugs. *ADME-Tox Approaches* **5:** 193-214

Olsson B, Bondesson E, Borgström L, Edsbäcker S, Eirefelt S, Ekelund K, Gustavsson L, Hegelund-Myrbäck T (2011) Pulmonary drug metabolism, clearance, and absorption. In *Controlled pulmonary drug delivery*, pp 21-50. Springer

Omiecinski CJ, Heuvel JPV, Perdew GH, Peters JM (2011) Xenobiotic metabolism, disposition, and regulation by receptors: from biochemical phenomenon to predictors of major toxicities. *Toxicological Sciences* **120:** S49-S75

Oyama T, Sugio K, Uramoto H, Iwata T, Onitsuka T, Isse T, Nozoe T, Kagawa N, Yasumoto K, Kawamoto T (2006) Increased cytochrome P450 and aryl hydrocarbon receptor in bronchial epithelium of heavy smokers with non-small cell lung carcinoma carries a poor prognosis. *Frontiers in bioscience: a journal and virtual library* **12:** 4497-4503

Patel M, Lu L, Zander DS, Sreerama L, Coco D, Moreb JS (2008) ALDH1A1 and ALDH3A1 expression in lung cancers: correlation with histologic type and potential precursors. *Lung Cancer* **59:** 340-349

Pavek P, Dvorak Z (2008) Xenobiotic-induced transcriptional regulation of xenobiotic metabolizing enzymes of the cytochrome P450 superfamily in human extrahepatic tissues. *Current drug metabolism* **9:** 129-143

Pelkonen O, Kapitulnik J, Gundert-Remy U, Boobis A, Stockis A (2008) Local kinetics and dynamics of xenobiotics. *Critical reviews in toxicology* **38:** 697-720

Penning TM, Lerman C (2008) Genomics of smoking exposure and cessation: lessons for cancer prevention and treatment. *Cancer Prevention Research* **1:** 80-83

Petrash M (2013) The role of human aldo-keto reductases in the metabolic activation and detoxication of polycyclic aromatic hydrocarbons: interconversion of PAH catechols and PAH or quinones. *Aldo-keto reductases and role in human disease***:** 36

Phillips B, Esposito M, Verbeeck J, Boué S, Iskandar A, Vuillaume G, Leroy P, Krishnan S, Kogel U, Utan A (2015a) Toxicity of aerosols of nicotine and pyruvic acid (separate and combined) in Sprague–Dawley rats in a 28-day OECD 412 inhalation study and assessment of systems toxicology. *Inhalation toxicology* **27:** 405-431

Phillips B, Veljkovic E, Boué S, Schlage WK, Vuillaume G, Martin F, Titz B, Leroy P, Buettner A, Elamin A, Oviedo A, Cabanski M, Guedj E, Schneider T, Talikka M, Ivanov NV, Vanscheeuwijck P, Peitsch MC, Hoeng J (2015b) An 8-Month Systems Toxicology Inhalation/Cessation Study in Apoe-/- Mice to Investigate Cardiovascular and Respiratory Exposure Effects of a Candidate Modified Risk Tobacco Product, THS 2.2, Compared with Conventional Cigarettes *Toxicological Sciences* **In press**

Price RJ, Renwick AB, Walters DG, Young PJ, Lake BG (2004) Metabolism of nicotine and induction of CYP1A forms in precision-cut rat liver and lung slices. *Toxicology in vitro* **18:** 179-185

Ren Q, Murphy SE, Zheng Z, Lazarus P (2000) O-Glucuronidation of the lung carcinogen 4-(methylnitrosamino)-1-(3-pyridyl)-1-butanol (NNAL) by human UDP-glucuronosyltransferases 2B7 and 1A9. *Drug Metabolism and Disposition* **28:** 1352-1360

Roos PH, Bolt HM (2005) Cytochrome P450 interactions in human cancers: new aspects considering CYP1B1. *Expert opinion on drug metabolism & toxicology* **1:** 187-202

Runge DM, Stock TW, Lehmann T, Taege C, Bernauer U, Stolz DB, Hofmann S, Foth H (2001) Expression of cytochrome P450 2E1 in normal human bronchial epithelial cells and activation by ethanol in culture. *Archives of toxicology* **75:** 335-345

Rylander T, Neve EP, Ingelman-Sundberg M, Oscarson M (2001) Identification and tissue distribution of the novel human cytochrome P450 2S1 (CYP2S1). *Biochemical and biophysical research communications* **281:** 529-535

Sagredo C, Øvrebø S, Haugen A, Fujii-Kuriyama Y, Bæra R, Botnen IV, Mollerup S (2006) Quantitative analysis of benzo [a] pyrene biotransformation and adduct formation in Ahr knockout mice. *Toxicology letters* **167:** 173-182

Scheffer G, Pijnenborg A, Smit E, Müller M, Postma D, Timens W, Van Der Valk P, De Vries E, Scheper R (2002) Multidrug resistance related molecules in human and murine lung. *Journal of clinical pathology* **55:** 332-339

Schlage WK, Westra JW, Gebel S, Catlett NL, Mathis C, Frushour BP, Hengstermann A, Van Hooser A, Poussin C, Wong B (2011) A computable cellular stress network model for non-diseased pulmonary and cardiovascular tissue. *BMC systems biology* **5:** 168

Shigenaga M, Trevor A, Castagnoli N (1988) Metabolism-dependent covalent binding of (S)-[5-3H] nicotine to liver and lung microsomal macromolecules. *Drug metabolism and disposition* **16:** 397-402

Somers GI, Lindsay N, Lowdon B, Jones A, Freathy C, Ho S, Woodrooffe A, Bayliss M, Manchee G (2007) A comparison of the expression and metabolizing activities of phase I and II enzymes in freshly isolated human lung parenchymal cells and cryopreserved human hepatocytes. *Drug Metabolism and Disposition* **35:** 1797-1805

Su T, Bao Z, Zhang Q-Y, Smith TJ, Hong J-Y, Ding X (2000) Human cytochrome P450 CYP2A13: predominant expression in the respiratory tract and its high efficiency metabolic activation of a tobacco-specific carcinogen, 4-(methylnitrosamino)-1-(3-pyridyl)-1-butanone. *Cancer Research* **60:** 5074-5079

Su T, Sheng JJ, Lipinskas TW, Ding X (1996) Expression of CYP2A genes in rodent and human nasal mucosa. *Drug metabolism and disposition* **24:** 884-890

Thomas G, Barrand M, Stewart S, Rabbits P, Williams E, Twentyman P (1994) Expression of the multidrug resistance-associated protein (MRP) gene in human lung tumours and normal tissue as determined by in situ hybridisation. *European Journal of Cancer* **30:** 1705-1709

Thum T, Erpenbeck VJ, Moeller J, Hohlfeld JM, Krug N, Borlak J (2006) Expression of xenobiotic metabolizing enzymes in different lung compartments of smokers and nonsmokers. *Environmental health perspectives***:** 1655-1661

van der Deen M, De Vries E, Timens W, Scheper RJ, Timmer-Bosscha H, Postma DS (2005) ATP-binding cassette (ABC) transporters in normal and pathological lung. *Respir Res* **6:** 59

van der Deen M, Marks H, Willemse BW, Postma DS, Müller M, Smit EF, Scheffer GL, Scheper RJ, de Vries EG, Timens W (2006) Diminished expression of multidrug resistance-associated protein 1 (MRP1) in bronchial epithelium of COPD patients. *Virchows Archiv* **449:** 682-688

Vasiliou V, Thompson DC, Smith C, Fujita M, Chen Y (2013) Aldehyde dehydrogenases: from eye crystallins to metabolic disease and cancer stem cells. *Chemico-biological interactions* **202:** 2-10

Wang X, Hu J-F, Tan Y, Cui J, Wang G, Mrsny RJ, Li W (2014) Cancer stem cell marker Musashi-1 rs2522137 genotype is associated with an increased risk of lung cancer. *PloS one* **9:** e95915

Weng Y, Fang C, Turesky RJ, Behr M, Kaminsky LS, Ding X (2007) Determination of the role of target tissue metabolism in lung carcinogenesis using conditional cytochrome P450 reductase-null mice. *Cancer Research* **67:** 7825-7832

Xu M, Ju W, Hao H, Wang G, Li P (2013) Cytochrome P450 2J2: distribution, function, regulation, genetic polymorphisms and clinical significance. *Drug metabolism reviews* **45:** 311-352

Zhang JY, Fen Wang Y, Prakash C (2006) Xenobiotic-metabolizing enzymes in human lung. *Current drug metabolism* **7:** 939-948

Zhang L, Lee JJ, Tang H, Fan Y-H, Xiao L, Ren H, Kurie J, Morice RC, Hong WK, Mao L (2008) Impact of smoking cessation on global gene expression in the bronchial epithelium of chronic smokers. *Cancer Prevention Research* **1:** 112-118